ČESKÉ VYSOKÉ UČENÍ TECHNICKÉ V PRAZE

FAKULTA JADERNÁ A FYZIKÁLNĚ INŽENÝRSKÁ

KATEDRA MATERIÁLŮ

Tepelná stabilita wolframových slitin

DISERTAČNÍ PRÁCE

Ing. Jakub Veverka

Studijní program :	Aplikace přírodních věd
Studijní obor :	Fyzikální inženýrství
Zaměření :	Stavba a vlastnosti materiálů

Školitel :

Ing. Ondřej Kovářík, Ph.D. / ČVUT FJFI KMAT

Školitel – specialista :

Ing. Monika Vilémová, Ph.D. / ÚFP AV ČR

Datum vydání : 28.02.2023 *Pořadové číslo výtisku : 1*

Czech Technical University in Prague
Faculty of Nuclear Sciences and Physical Engineering
Department of Materials

Thermal stability of tungsten alloys

Doctoral thesis

Ing. Jakub Veverka

Study Program: Application of Natural Sciences
Branch of study: Physical Engineering
Specialization: Materials Structure and Properties

Prague 2023

Bibliografický záznam

Autor:	Ing. Jakub Veverka České vysoké učení technické v Praze Fakulta jaderná a fyzikálně inženýrská Katedra materiálů
Název práce:	Teplotní stabilita wolframových slitin
Studijní program:	Aplikace přírodních věd
Studijní obor:	Fyzikální inženýrství
Školitel:	Ing. Ondřej Kovářík, Ph.D. České vysoké učení technické v Praze Fakulta jaderná a fyzikálně inženýrská Katedra materiálů
Školitel-specialista:	Ing. Monika Vilémová, Ph.D. Ústav fyziky plazmatu AV ČR, v.v.i. Oddělení materiálového inženýrství
Akademický rok:	2022/2023
Počet stran:	94
Klíčová slova:	spark plasma sintering, wolfram-chromové slitiny, wolfram, tuhý roztok, stabilizace, *ab-initio* modelování

Bibliographic entry

Author:	Ing. Jakub Veverka Czech Technical University in Prague Faculty of Nuclear Sciences and Physical Engineering Department of Materials
Title of Dissertation:	Thermal stability of tungsten alloys
Degree program:	Application of Natural Sciences
Field of study:	Physical Engineering
Supervisor:	Ing. Ondrej Kovarik, Ph.D. Czech Technical University in Prague Faculty of Nuclear Sciences and Physical Engineering Department of Materials
Supervisor-Specialist:	Ing. Monika Vilemova, Ph.D. The Czech Academy of Sciences, Institute of Plasma Physics Department of Materials Engineering
Academic Year:	2022/2023
Number of Pages:	94
Keywords:	spark plasma sintering, tungsten-chromium alloys, tungsten, solid solution, stabilisation, *ab-initio* modelling

Acknowledgements

I would like to express my greatest gratitude to my supervisor-specialist, Monika Vilémová, for her guidance, help with the experimental setups, numerous consultations and manuscript reviews, including a significant number of research tips for future career. I would like to also thank my supervisor, Ondřej Kovářík, for the assistance with various formal issues regarding the study and thesis, valuable tips regarding the experiments and for reviewing the manuscripts and thesis. I would also like to thank to all respective co-authors of the journal articles for their help in creating this thesis. Special thanks belong to the colleagues from IT4Innovations, for the opportunity to employ their supercomputer capacity and valuable consultations regarding theoretical calculations. Last but not least I would like to thank all my colleagues, permanent or visiting, from the Materials Engineering and Laboratory of Plasma Technologies of the IPP for invaluable help during my research, especially: Zdeněk Dlabáček for SPS samples production, Fero Lukáč for numerous XRD analyses, Radek Mušálek for critical equipment training, Honza Medřický and Kuba Klečka for technical assistance, and Tom Tesař for setting the peer-pressure with his own PhD. All the above mentioned also deserve many thanks for such incredible atmosphere in the ME Department.

Significant amount of experimental work presented in this thesis was supported by the Czech Science Foundation through grant No. 20-18392S, which is gratefully acknowledged.

Declaration

I hereby declare that this doctoral thesis is my original work and that the sources used within are provided in the list of references in accordance with the Methodological Instructions on Ethical Principles in the Preparation of University Theses.

I also declare that I wrote all the original research articles that are presented in the experimental part of the thesis, with the help of co-authors listed herein.

In Prague, February, 2023

Abstract

Thermonuclear fusion is an essential part of future energetic mix, in order to cope with increasing humanity energy demands, shortage of resources and environmental burden of fossil fuels. Although some parts of the already established infrastructure for nuclear power plants can be adopted, due to different nature of the energy producing reaction, the key components must be developed entirely new. The research has been focused on controlled thermonuclear fusion already since 1950s and theoretically the issue is covered well, including parameter design of the facility, which should be capable of achieving energy gain. This facility is nowadays completed from about 80 % and is supposed to be commissioned during next five years. Again, due to the physics, conditions for achieving thermonuclear reaction on Earth are much more stringent compared to nuclear fission, especially the required temperature – 150-200 million Kelvin. Strong magnetic field, high mechanical force, heat, and particle fluxes in the facilities put significant demands on the materials for internal components. The material range is broad due to many different applications to be fulfilled; however, the main concern has been with the materials being directly exposed to plasma. This material group is frequently labelled as “plasma facing materials”, being the construction materials of “plasma facing components - PFCs”. Although the operation will be performed in vacuum, to lower the plasma heat losses, still the PFCs will suffer from significant heat fluxes, resulting from the great temperature gradient. Resulting surface temperature may exceed melting point of most of the metals, therefore the research interest was focused on tungsten based materials, alloys or composites. Such materials have sufficient thermal properties; however, there are other issues to be solved, e.g., mechanical properties. Also, considering the future nuclear devices, safety is an essential issue, especially in light of the few nuclear power plants accidents which still affect the public opinion. In that way, tungsten based materials suffer from inherently low oxidation resistance and high sublimation rate of tungsten oxides. Because of the significant neutron flux, produced during the fusion reaction, the PFCs will become activated during the operation. This might be avoided in advanced fusion facilities, but in the first generation power plants, the least complicated reaction must be harnessed. In case of possible breach of reactor integrity, the tungsten components will oxidize, and the oxides might be released into outer environment, resulting in significant and widespread radiation contamination. Because of that, research is focused on development of tungsten alloys which improve this behaviour by

forming thin surface oxide layer, preventing tungsten oxidation and subsequent sublimation, i.e., preventing the radiation contamination in case of accident. In this thesis, the problematics of tungsten-based alloys with passivation properties is explored. Major element responsible for the passivation is chromium; however, the miscibility with tungsten is limited. Therefore, non-equilibrium fabrication methods must be used, to first get the powder material and later a solid sample as well. This problematic is covered by literature review, as well as experimentally, in the journal articles. Different alloying elements were pursued and significant improvement in alloy stability, essential for successful application, was achieved. Later, the experiments were designed following the results of the computational model, capable of assessing the produced alloys/phases and their stability. During these studies, potential prospective way to prepare ultra-fine-grained composite materials with given elastic properties was also developed, along with the computational predictive model verified by experiment. Additional research was performed on the mechanical properties of base tungsten metal: exploring the influence of process parameters on basic impurity levels (carbon and oxygen), investigating the intake process, and evaluating the influence on ductility. These results were also published in the form of journal article.

Abstrakt

Termojaderná fúze je nezastupitelnou součástí energetického mixu, schopného vypořádat se s rostoucími energetickými nároky lidstva, ztenčujícími se přírodními zdroji a ekologickou zátěží fosilních paliv. Přestože lze pro tento energetický zdroj částečně využít již etablovanou infrastrukturu jaderných elektráren, množství komponent bylo třeba z důvodu odlišného fyzikálního principu vyvinout zcela znovu. Počátek výzkumu řízené termojaderné fúze se datuje do padesátých let minulého století a problematika je rozsáhle teoreticky popsána, včetně návrhu zařízení dosahujícího energetického zisku. Zmíněné zařízení se momentálně blíží hranici 80 procent dokončení a zahájení provozu se očekává během pěti let. Podmínky nutné pro zažehnutí jaderné fúze na Zemi se dramaticky liší od požadavků na jaderné štěpení, zejména co se týče teploty – je nutné dosáhnout 150-200 milionů stupňů. Silné magnetické pole, značné mechanické síly a vysoké tepelné i částicové toky znamenají vysoké namáhání materiálů vnitřních komponent reaktoru. Materiálové nároky fúzních zařízení jsou široké, kvůli množství podsystémů, nicméně největší důraz je kladen na materiály přímo vystavené plazmatu. Tato materiálová skupina je značována jako “plasma facing materials” a jsou základní součástí takzvaných “plasma facing components - PFCs”. Ačkoliv budou zařízení provozována při vakuu, za účelem snížení tepelných ztrát, PFCs budou stále vystaveny značným tepelným tokům, z důvodu ostrého teplotního gradientu. Povrchová teplota hrozí překročením teploty tání většiny kovových materiálů, proto se výzkum soustředí na wolfram, jeho slitiny nebo kompozity. Tyto materiály mají dostatečné tepelné vlastnosti, nicméně je třeba vyřešit některé jejich slabé stránky, například mechanické vlastnosti. Bezpečnost budoucích fúzních zařízení je zásadním tématem, zejména ve světle značného vlivu minimálního množství jaderných havárií na veřejné mínění. V tomto ohledu je slabinou materálů na bázi wolframu jejich nízká odolnost vůči oxidaci a vysoká míra sublimace oxidů wolframu. Kvůli značnému neutronovému toku, vznikajícímu při fúzní reakci, budou materiály PFCs během provozu aktivovány. V pozdějších generacích fúzních zařízení bude teoreticky možné se tomu vyhnout, nicméně nejsnáze dosažitelná fúzní reakce s sebou tento problém nese. V případě narušení integrity reaktoru pak existuje riziko oxidace wolframových částí a uvolnění značného množství radioaktivního prachu do okolí. Z tohoto důvodu se výzkum zaměřuje na vývoj wolframových slitin se schopností samopasivace, kdy je při vystavení oxidačnímu prostředí vytvořena tenká povrchová vrstva oxidu, zabraňující další hloubkové

oxidaci a zejména rozsáhlému radiačnímu zamoření. V rámci této disertační práce je rozpracovávána problematika wolframových slitin se samopasivačními vlastnostmi. Důležitým prvkem zajišťujícím pasivitu je chrom, nicméně jeho rozpustnost ve wolframu je omezená. Proto je třeba využít nerovnovážné metody přípravy, a to jak počátečního prášku, tak pevných vzorků. Tato problematika je zpracována jak formou literární rešerše, tak článků v impaktovaných časopisech. Bylo zkoumáno několik příměsových prvků a bylo dosaženo významného zlepšení stability slitiny. Pozdější experimenty byly plánované s využitím výsledků počítačového modelu, schopného analyzovat vzniklé faze a jejich stabilitu. V průběhu studie byla také vyvinuta metoda použitelná pro přípravu jemnozrnného (UFG) materiálu s definovanými elastickými vlastnostmi, včetně předpovědního počítačového modelu, ověřeného experimentem. Další směr výzkumu byl zaměřen na mechanické vlastnosti wolframu – vliv parametrů výrobního procesu na úrovně koncentrace nejdůležitějších nečistot (uhlíku a kyslíku), zkoumání jejich transport a vlivu na mechanické vlastnosti materiálu, zejména tažnost. Výsledky byly taktéž zpracovány do podoby impaktovaného článku.

Contents

List of abbreviations

BPR – ball to powder ratio

CANDU – Canada deuterium uranium, Canadian pressurized heavy-water nuclear reactor

DBTT – ductile to brittle transition temperature

DEMO – demonstrational fusion reactor

DPA – displacement per atom

EDM – electric discharge manufacturing

ELM – edge localised mode, plasma instability

FAST – field assisted sintering technique

FPY – full power year

HCPB – helium cooled pebble bed, one of tritium breeding blanket designs

IGP – ITER grade Plansee, specific industrial grade of tungsten

ITER – International thermonuclear reactor

LOCA – loss of coolant accident

MA – mechanical alloying

ODS – oxide dispersion-strengthened

PFCs – plasma facing components

PFM – plasma facing material

SEM – scanning electron microscopy

UTS – ultimate tensile strength

YS – yield strength

1. Introduction

Majority of today's energy is produced by burning fossil fuels – coal, natural gas and oil. These fuels are non-renewable, which means that they cannot be replenished at the mankind-relevant time scales. Moreover, the Earth population is growing, with increasing rate. Based on different simulations, at the beginning of new millennia the population at year 2100 was expected to be between 10 to 12 billion people. Similar increase was expected in the energy consumption as well, even more pronounced, because the average energy use is very inhomogeneous – for Africa, India or China, the average is about ten-fold lower than for the United States (see Figure 1 left). When countries with lower consumption aim to increase the life standard, the energy consumption by the year 2100 was expected to be two to five times higher than today (see Figure 1 right).

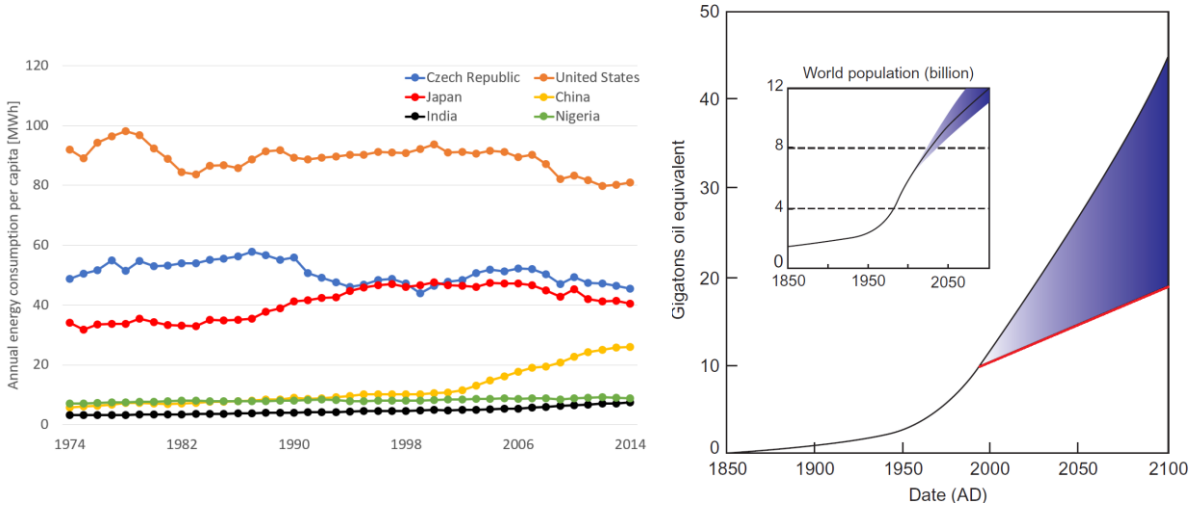

Fig. 1: Annual energy consumption per capita from 1974 to 2014 (left, plotted based on data from [1]), evolution of annual world energy consumption and world population (insert) with estimated projection till the year 2100 (right, modified according to [2]). 1 gigaton oil equivalent equals 11.63 PWh. Red line depicts most probable evolution of energy consumption based on recent advances in energetics.

Recent assessment led to re-evaluation of the predictions and although the population increase is expected to be similar, the improvements in efficiency and general policy of energy savings resulted in lower increase in energy demands. Still the global energy needs are supposed to expand by 30 % to year 2040 [3]. This would accelerate the production and consumption of fossil fuels. Today´s estimates set the remaining supplies of oil and gas to last only for several decades, for coal more than hundred years. However, this does not account for increased consumption. With increased fossil fuels consumption significant environmental issues are also associated - water pollution, deforestation, greenhouse gases production etc. Most pronounced is the greenhouse gases production, especially carbon dioxide. Broad consensus has been reached that CO_2 production increased significantly since the beginning of the Industrial Revolution – see Figure 2 left. In addition, CO_2 emissions are inhomogeneous in the same way as energy consumption, as can be seen from Figure 2 right. One can see, that although the annual CO_2 production of Czech Republic is almost 100 times lower compared to China (104 million to 9.8 billion tonnes for 2017 [4]), the production per capita is higher – almost by one half. The most populated countries, e.g. China and India have therefore potential for major increase of CO_2 production, which may have serious consequences.

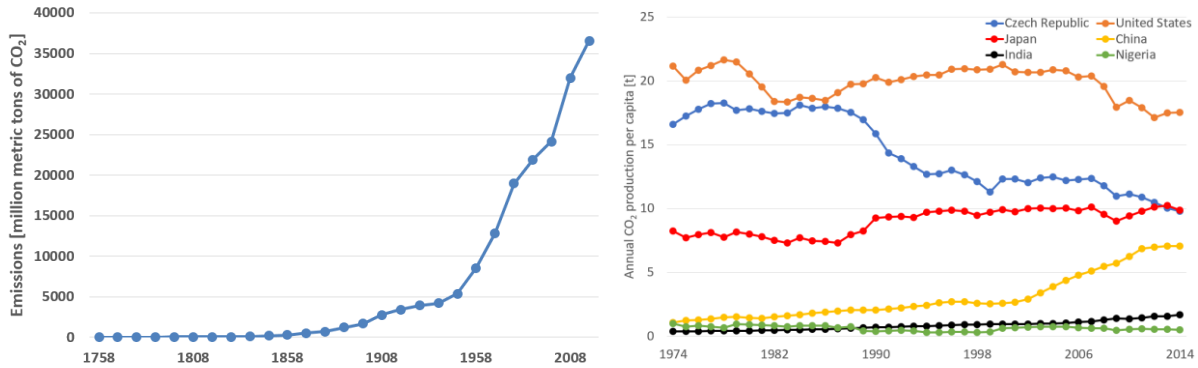

Fig. 2: Global annual carbon dioxide emissions from 1758 to 2018, fossil fuel combustion and industrial processes combined (left, plotted based on data from [5]), Annual carbon dioxide emissions per capita from 1974 to 2014 (right, plotted based on data from [4]).

Increasing amount of CO_2 in atmosphere amplifies global warming effect, resulting in significant climate changes. The report of the Intergovernmental Panel on Climate Change (IPCC) [6] from 2014 stated that global temperature increase of 1 °C compared to average temperature over 1850-1900 period has already been reached. The increase was expected to reach 1.5 °C between years 2030 and 2052 and probably up to 4 °C by 2100 at current increase rate. Climate models projected significant changes in weather extremes, precipitations, sea level increase etc. To limit the environmental consequences, the global effort to keep the temperature increase below 2°C and pursue efforts to limit the increase to 1.5 °C was adopted by the Paris Agreement [7]. The impacts would still be significant; however, not critical. To achieve the 2 °C goal, net zero CO_2 emissions must be achieved until 2070, for 1.5 °C until 2055 [6]. However, presented predictions dealt also with possibility of temporary overshooting of the 1.5 °C limit. The updated report [8] was published in 2021 and stated that in comparison to 1850-1900 period, global surface temperature between 2011 and 2020 was higher by 1.09 °C (1.59 °C for temperature above the land and 0.88 °C above the ocean). Also, since 1970 the global surface temperature has increased faster than in any other 50-year period over at least the last 2000 years. Regarding future predictions, 5 different scenarios were presented, based on the levels of CO_2 emissions and other greenhouse gases (GHG) emissions. The scenarios span from the worst-case, expecting almost doubled CO_2 emissions by 2050 or 2100, to best-case with net zero emissions around 2050. However, under all considered scenarios, global surface temperature will continue to increase until approximately 2060s, overshooting the 1.5 °C limit and very likely even 2 °C. Only under scenarios facilitating deep reductions of emissions, the increase in temperature under 2 °C around 2100 can be achieved. Projected values of temperature change can be seen in the figure 3. This corresponds with the predictions of World Meteorological Organization, which suggest that the annual mean global temperature will be at least 1 °C higher in each of the coming 5 years (2021-2025) and is very likely to be between 0.9 – 1.8 °C higher, compared to 1850-1900 period [9]. Also it is almost certain (90 % probability) that at least one of these years will exceed the temperature record from 2016 and there is about 40 % probability that at least one year will be 1.5 °C warmer than 1850-1900 period. Such temperature increase is expected to be accompanied by severe climate changes, e.g. by increase in frequency and intensity of hot temperature extremes.

According to [8], for 2 °C temperature increase, 10-year extreme temperature event will occur 6 times during 10 years (compared to 3 times nowadays), with approximately 1.4 °C temperature increase from present values.

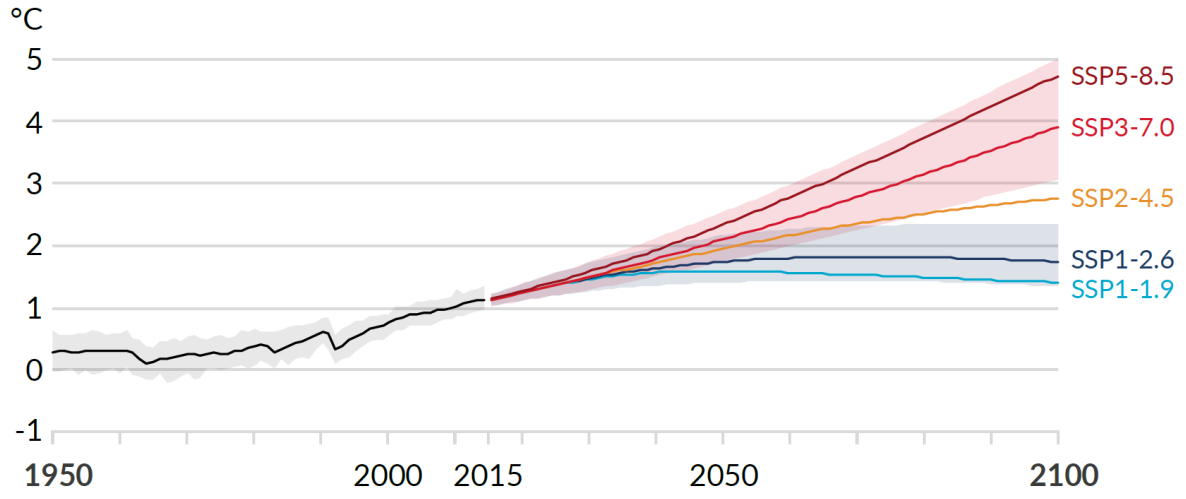

Fig. 3.: Predictions of global temperature change relative to pre-industrial era for different scenarios of CO_2 emissions mitigation, modified according to [8]. Shaded areas correspond to SSP1-2.6 (low GHG and net zero CO_2 emissions) and SSP3-7.0 (high GHG and 50% higher CO_2 emissions) scenario, respectively.

As energy production from fossil fuels is major contributor to CO_2 emissions, alternative means of production must be employed to achieve these ambitious goals. However, sufficient energy supply for the population and industry must be sustained. Broad spectrum of renewable energy sources has been explored, e.g. solar photovoltaic, hydroelectricity or wind power; however, there still is number of issues to be resolved if renewables should constitute major share of energy sources. Electricity output from solar and wind power is unstable, affecting the grid stability and reliability. The output is often lower than the name-plate capacity and backup power plants, mainly fossil fuel based must be used. Those will have to operate at stand-by mode, delivering power according to the momentarily demand. Such operation leads to lower power plant thermal efficiency. Moreover, combined cost of primary and backup power plant including fuel and maintenance will likely exceed cost of fossil fuel-

based power plant [10]. On the other hand, eventual overproduction during periods of suitable conditions and low demand cannot be stored effectively yet. Efficiency of photovoltaic panels is limited by operating temperature, analogously wind turbine efficiency is limited by wind speed. Large areas or specific landscape is required for effective use of hydroelectricity. In addition, some studies claim that effective mitigation of CO_2 emissions is not reached until share of renewable energy sources exceeds certain level (about 8.5 % in [11]). Nevertheless, with improved output stability and storage efficiency, renewable energy sources can become vital part of the energetic mix. Based on the development in Asian countries, mainly China and India, it is estimated that by year 2040 renewable energy sources would account for 40 % of production. In the European Union, renewables constitute 80 % of newly installed capacity [3]. However, complete transition to renewable energy sources does not seem to be viable universal solution, due to production instability and material demands.

Nuclear energy (fission) could be viable alternative, effectively mitigating several drawbacks of renewable sources while maintaining zero CO_2 emissions. It is both scientifically and technologically proven means of energy, capable of delivering huge amount of power reliably, as can be seen for example in France, as over 75 % of electricity is produced by nuclear power plants. Yet the electricity price and per-capita emissions of greenhouse gasses are among the lowest worldwide [10]. In addition, price of fission electricity is much less sensitive to fuel price increase, i.e. uranium, in contrast to fossil fuel-based power plants. Conservative estimates of uranium supplies for up-to-date nuclear power plants, i.e. fissile uranium isotope U-235 are usually quoted to be sufficient for approximately 300 years [12]. However, fast-neutron fission reactors capable of utilizing also more abundant isotope U-238 and other subsequent transmutation products are already scientifically proven concepts, which need to be made commercially available. Such reactors can extract up to 100 times more energy from the fuel, therefore the supplies should be sufficient for several tens of thousands of years [13]. Naturally there are several safety and environmental issues which must be covered. Radiation safety must be ensured both during and after the end of operation. Certain power plant components will become strongly radioactive and must be stored together with spent nuclear fuel for certain period of time after end of operation. However, recently developed and tested recycling method allowed to reduce the waste volume as well as required storage time –

instead of thousands or hundreds of thousands of years, several hundred years should be enough to lower the radiation level below natural background values. Substituting fossil fuel-based power plants also prevents significant CO_2 emissions and dispersion of other harmful materials. Coal-fired power plants are able to emit more radioactive material than actual fission power plants [14]. In addition, average mortality rates per billion kWh are substantially lower for nuclear power plants than for other means of electricity production including renewable resources [10]. However, massive construction of new nuclear (fission) power plants is questionable as public opinion is rather anti-nuclear following several incidents, most recently Fukushima-Daichi accident, although the consequences on public health were not nearly as severe as those of fossil fuels.

Nuclear fusion has been proposed for decades as a promising energy source, considering its enormous fuel resources, no CO_2 emissions and inherently safe operation, supported by use of low activation elements and fuel with short half-life. In the first generations of power plants, fusion of hydrogen isotopes deuterium and tritium will be used, so called D-T reaction. Deuterium can be filtered from water and therefore, considering enormous supply of water on Earth (as sea water can be used for extraction), the reserves are inexhaustible on relevant timescales. Tritium can be produced directly in the reactor by fission of lithium, which is beneficial regarding the nuclear material transport, which will occur only in closed loop inside the power plant. Lithium itself is 25th most abundant element in Earth´s crust and also seawater content of lithium is very large. Therefore, the fuel supplies are sufficient for thousands of years, until advanced fusion reactions will be harnessed, or the human civilization will perish. In addition, the exhaust product of D-T reaction is helium – noble gas which can be either further used (for cooling purposes or as protective atmosphere) or released into the atmosphere without harmful effects. Nevertheless, there are several technological difficulties, e.g. reaching and maintaining very high plasma temperature, preventing plasma instabilities, high heat and neutron loads on the components etc. Required temperatures are in the range of several hundred million degrees, which is demanding task. At such temperatures, significant amount of heat is also radiated from the plasma, which requires operation in vacuum. Increasing the temperature over certain point also triggers instabilities in plasma, which is then difficult to confine in safe position. Heat loading issues

are most pronounced for the so-called Plasma Facing Components (PFCs). These components are the closest physical boundary to the plasma, in some cases plasma particles reach directly the components´ surface. Therefore, excellent heat flux resistant and low activation materials are required in order to harvest energy by nuclear fusion.

2. Nuclear fusion

Nuclear fusion is a reaction during which two lighter atomic nuclei merge and form one heavier. Additional particles may be released as well, depending on the reaction. The total binding energy of the heavier nucleus is greater than the sum of the binding energies of the original nuclei, therefore the remaining energy is released. This declares the possibility of energy production by fusion and is confirmed by the observations – nuclear fusion is a process responsible for energy production of stars in the whole universe. On the contrary to fission, the conditions for reaching the fusion are significantly more difficult, as the merging nuclei are of the same electric charge and the repulsive forces are tremendous. Energy sufficient to overcome these forces is usually acquired by heating the matter to high temperatures, reaching up to several million degrees (in space) or several hundreds of million degrees (on the Earth). Hence the nuclear fusion is frequently mentioned as thermonuclear fusion. The main reasons for the temperature difference are way of confinement and reaction chosen for achieving. During beginning of fusion research in 1950s it was discovered that for achieving fusion reaction, sufficient amount of fuel must be kept at certain temperature for sufficient time [15]. Product of these three quantities must be higher than certain critical value, different for particular reaction. In space, e.g. in the Sun, enormous mass is confined by gravitational force. Based on previously mentioned theory, with the large mass and long-term stability of Sun, the temperatures can be lower. As the gravitational confinement is not feasible on the Earth, other means must be involved e.g. magnetic. The confined mass is then much smaller; therefore, the temperature must be higher. In addition, the Sun produces energy through the so-called pp cycle, fusing protons into hydrogen and subsequently helium. This reaction is extremely slow – it takes about 10^9 years for average proton to fuse in the Sun, therefore other reactions must be employed for controlled fusion on the Earth [16]. Hydrogen isotope fusion is the least demanding and the maximum cross-section (measure of probability of particles' collision) is reached for deuterium and tritium fusing, in the range of 200-300 million Kelvin. This reaction will therefore be harnessed in the first generation of fusion power plants. Stable confinement of the plasma at such high temperatures is very challenging and still has not been routinely achieved.

On the other hand, fusion has several advantages over the fission and other means of electricity production, such as:

- Inherently safe reaction

  Fusion reaction is not a chain reaction like fission. Continuous fuelling is required to keep the reaction, amount of fuel simultaneously present in the reactor is several grams. Uncontrolled power increase is therefore impossible. High and fast temperature increase triggers several plasma instabilities, resulting in energy loss and termination of fusion reaction. Presence of any impurities potentially caused by a loss of reactor integrity would lead to the same effect.

- Short-term radioactive waste

  On the contrary to fission reactors, no spent fuel will be generated from fusion power plants. All reactants will be consumed, and, in first generation facilities, helium will be left as waste product. Certain reactor components will become activated due to neutron production or tritium presence. However, the level of neutron-induced radioactivity can be lowered by using low activation materials. In addition, tritium has half-life of ca. 12 years, therefore does not constitute serious threat during decommissioning.

- Environment friendly energy source

  Compared to fossil fuels, majority of fuel does not need to be mined – deuterium can be extracted by filtering sea water. Lithium will be mined; however, in significantly lower quantities and with lower environmental hazards. The operation is then entirely without harmful exhaust gasses such as carbon dioxide, sulphur trioxide etc., commonly present during fossil fuels combustion.

- Vast and more equally distributed fuel reserves

  Fuel for the first-generation facilities will be hydrogen isotopes, deuterium and tritium. Deuterium can be filtered in high amount from the sea water, tritium can be in-situ produced by fission of lithium or supplied in limited amount from CANDU fission reactors. Supply of both sources can last for many generations until advanced fusion reactions are facilitated. In addition, the reserves are distributed more equally around the globe, compared to oil, for example.

- Higher specific energy density

  Fusing of hydrogen nuclei releases substantially higher amount of energy for equal mass involved compared to fossil fuel combustion – about four million times more. Even compared to fission, the release is higher – about four times [17]. This constitutes one of the major advantages, in conjunction with the enormous fuel reserves.

3. Tokamak structure and operation conditions

To achieve the fusion successfully, new type of nuclear reactor must be developed. From several concepts, tokamak has reached the best results so far and has been chosen both for the ITER project, first thermonuclear facility that should reach energy profit from fusion reaction, and DEMO, demonstrational power plant. Comparison of key parameters of these facilities and expected values for actual fusion reactor for electricity production (e.g. no scientific experiments) is displayed in Table 1.

	ITER	DEMO	*Reactor*
Fusion Power	**0.5 GW**	**2 – 2.5 GW**	***3 - 4 GW***
Heat flux (FW)	**0.1-0.3 MW/m^2**	**0.5 MW/m^2**	***0.5 MW/m^2***
Neutron Wall Load (First Wall)	**0.78 MW/m^2**	**< 2 MW/m^2**	***~ 2 MW/m^2***
Integrated wall load (First Wall)	**0.07 MW.year/m^2 (3 years Inductive operation I)**	**5 - 8 MW.year/m^2**	***10 - 15 MW.year/m^2***
Displacement per atom (dpa)	**< 3 dpa**	**50 - 80 dpa**	***100 - 150 dpa***

Tab. 1: Comparison of key parameters of ITER, DEMO and Fusion Reactor (first facility beyond DEMO dedicated solely to electricity production), modified according to [35].

Tokamak is a toroidal (doughnut-shaped) reactor, where the fuel is maintained in plasmatic state and confined by strong magnetic field. The main components of tokamak are shown in Figure 4: vacuum vessel, magnetic field coils and the Plasma Facing Components (PFCs) – divertor and first wall (outermost part of blanket modules). Plasma facing components are specific parts of the fusion reactor, which protect the vacuum vessel against heat and particle loads. The PFCs are divided into two groups – divertor and first wall. Divertor is a special component at the bottom of the vacuum vessel, where energetic particles from edge plasma are deflected (for detailed information see section 3.1). First wall is top part of the blanket modules, which are covering the rest of vacuum vessel surface (for detailed information see section 3.2).

During the operation PFCs will be exposed to significant heat flux both from the plasma radiation and particle fluxes. The steady-state heat loading at DEMO can reach up to 10 MW/m^2 with peak values of over 20 MW/m^2 during transient events [18]. Due to the heat loading, properties of material can change significantly, e.g. thermal conductivity, as well as yield and ultimate tensile strength can decrease [19]. Excessive heat loading can also result in recrystallization of material, leading to surface cracking and further degrading mechanical properties, e.g. increasing DBTT, decreasing hardness [20], strength [21] etc.

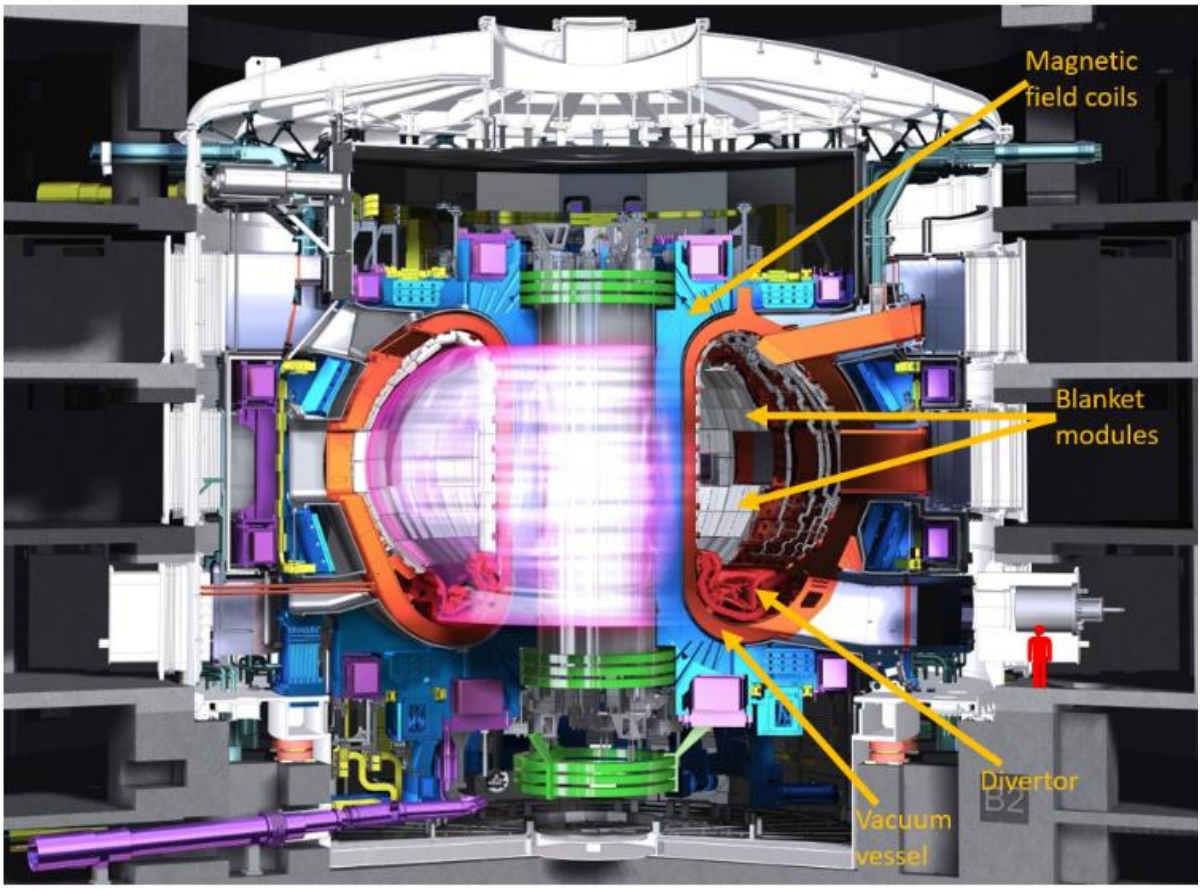

Fig. 4: Cross-section of the ITER reactor with the main components highlighted (modified according to [22]*). Presence of plasma is indicated by pink colour in the middle of the figure. Person to scale in the bottom right corner.*

Plasma facing material will be exposed to significant particle fluxes as well: neutrons, as well as ions and neutral atoms. While exposure to ions and neutrals will result mostly in sputtering and erosion, neutron flux will result in significant radiation damage. Radiation damage is

commonly assessed by dpa quantity referring to “displacement per atom”. At 1 dpa, each atom is knocked out of its original position once during the component lifetime. Simulations of DEMO neutron loading in [23] showed that the PFCs will be exposed to neutron fluxes of 10^{18} neutrons/(m^2·s) with significant proportion of 12-15 MeV neutrons, corresponding to armour damage levels of up to 9 dpa per full power year (fpy). Under such immense radiation, material properties can be changed significantly, e.g. by decrease of fracture toughness and ductility [24][25] or by decrease of thermal conductivity [26]. Considering the fluxes of ions and neutral atoms, additional flux of 10^{16} – 10^{18} particles/ (m^2·s) is expected [27]. Corresponding erosion rate is 10^{-2} – 10^{0} mm/fpy. In addition, the plasma facing materials will become activated. Consequences are two-fold: maintenance must be remote and decommissioning after the end of operation can be very long. The dose rate limit for hands-on recycling is usually set as 10^{-5} Sv/h, while for the remote recycling as 10^{-2} Sv/h [28]. With advanced remote handling equipment acceptable dose rate of up to 10^{3} Sv/h is proposed [29]. Thus, the aim of alloying is also to enhance irradiation and sputtering resistance of the material. However, all future fusion facilities designs expect that the hands-on limit is reached within 100 years after the reactor shutdown.

Last, but not least the material will be affected by gaseous hydrogen as well. Hydrogen isotopes have high solubility and diffusivity in metals, i.e. they can easily penetrate even intact bulk material and significant amount of hydrogen can be trapped in certain materials. Material properties can be worsened by hydrogen inventory, e.g. loss of ductility can occur [30], fatigue crack growth can be accelerated [31] and blistering or hydrogen bubble growth may occur [32]. In addition, in case of tritium used in fusion facilities, radiation safety must also be considered, although by current assumptions the inventory in PFCs will be minor. Total inventory in DEMO facility is estimated to be ca. 2 kg of tritium, while the vacuum vessel will account for several grams [33]. Such low values are ascribed to omitting in-vessel components containing carbon. Rest of tritium would be located in the breeding blanket systems, fuel clean-up, storage and delivery system, pumping system etc. ITER vacuum vessel safety limit was set as 350 g [34] and same magnitudes are assumed for DEMO. Therefore, hydrogen inventory should not be of concern regarding the radiological hazards, but rather material properties degradation.

3.1. Divertor

Divertor is located at the bottom of the vacuum vessel. Location and structure of divertor is displayed in Figure 5. Position of plasma facing material is marked by red arrows.

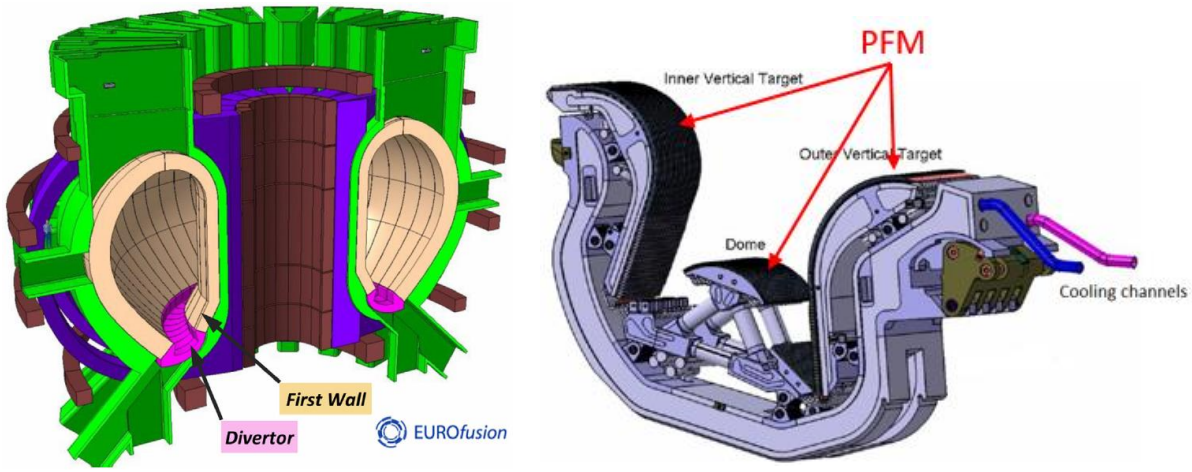

Fig. 5: Plasma facing components (PFC, left [40]), scheme of divertor structure with plasma facing material (PFM) indicated by arrows (right, modified according to [41]).

As the tokamak main magnetic field is circular and is generated in the cross-section of the vessel, at certain point, the outer field lines intersect the divertor target plates. Edge plasma particles following these lines will then be directed straight to the divertor. The primary function of divertor is to protect the vacuum vessel against these high energetic particles, to extract the deposited heat and to exhaust the gaseous impurities, mainly helium as the fusion reaction product. The steady-state heat flux for DEMO divertor is expected to reach 5-10 MW/m^2, with possible increase up to 20 MW/m^2 during the transient events [18]. According to Giancarli et al. [36] minimum temperature expected in divertor armour layer during steady state operation is estimated around 400 °C. This was also confirmed during high heat flux testing of divertor mock-ups [37]. For heat flux corresponding to steady-state operation, temperature of 600-900 °C was measured, for transient events the temperature has risen up to 1600-1900 °C. In case of unmitigated disruptive instability (ELM – edge localised mode), temperature can rise for very short time up to ca. 6000 °C [38]. However, systems for ELM mitigation are routinely implemented nowadays and such situations will be extremely rare. In

addition, neutron fluxes of 3-7·10^{18} neutrons/(m^2·s) are expected at divertor, depending on the position. Corresponding radiation damage of 6-7 dpa per full power year is expected, for the less exposed parts 2-3 dpa [23]. For actual fusion power plants, the cumulative damage of 150-200 dpa is expected, which is significantly higher than for current fission reactors - 70 dpa [39].

3.2. First wall

First wall is composed of number of panels at the top of the breeding blanket modules, installed on the inner surface of the vacuum vessel. These will be used for shielding the vacuum vessel against the heat and particle loads, extraction of deposited heat and in-situ tritium production. Structure and location of the first wall is displayed in detail in Figure 6 (one of the considered concepts). Position of plasma facing material is marked by red arrows.

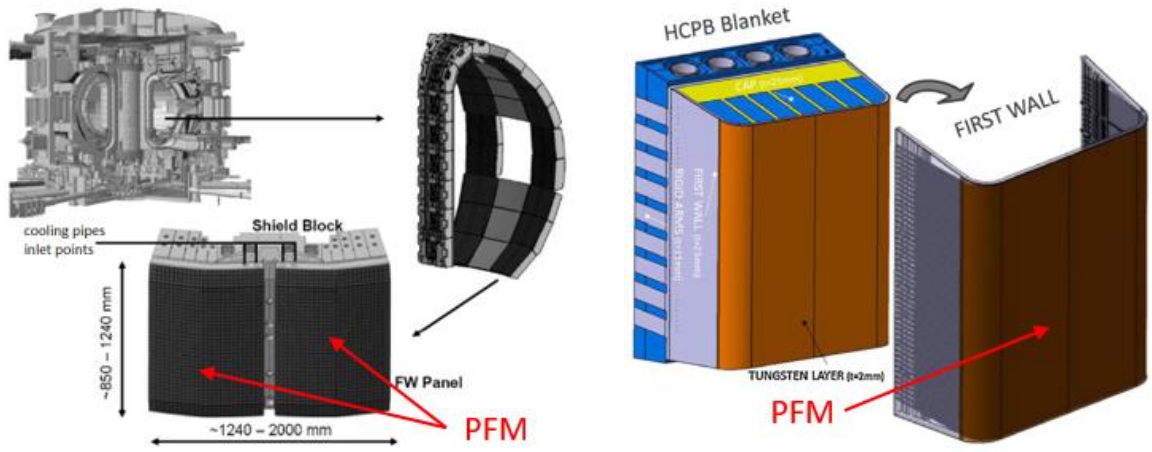

Fig. 6: Location and configuration of first wall shielding panels (left, modified according to [46]) and blanket modules (right, modified according to [40]). Plasma facing material, located on top surface of plasma facing components (shielding panel, blanket module etc.), is indicated by arrows. The figure depicts one of the considered concepts of the first wall design for European DEMO facility.

Radiation damage of the DEMO first wall will be greater than that of divertor, the simulations showed neutron fluxes of 8·10^{18} neutrons/(m^2·s) and damage of ca. 9 dpa per full power year [23]. On the other hand, heat flux is lower than at divertor: during the steady-state operation

0.3 MW/m^2 is expected [42]. Depending on the first wall design and blanket module location (heat flux deviates slightly around the vacuum vessel) peak heat loads during transient events or start-up could reach up to 1.2 MW/m^2 [43]. Accordingly, during steady-state operation maximum first wall temperature should reach ca. 430 °C, depending on cooling systems parameters [44]. As it is lower than for divertor, mechanical and thermal properties of the material can be compromised in favour of the passive safety. During the transient events, the temperature could rise up to 1550 °C, in exceptional cases up to ca. 3800 °C [45].

4. Fusion safety and lifecycle of the PFCs

To ensure reliable and safe reactor operation, structural integrity of the plasma facing components is essential. Therefore; the materials must withstand the conditions described in the beginning of section 3. Low neutron activation and hydrogen retention can be controlled by a suitable element choice whereas degradation by heat loading can be hindered by materials with low DBTT, sufficient ductility, good thermal shock and fatigue resistance. To ensure viability of fusion facilities, the required component properties must be preserved for sufficient time: estimated PFCs lifetime is about 5 years for the ITER reactor [34] and for the facilities beyond ITER (demonstrational power plant DEMO and commercial reactors) the lifetime will rise up to 15 years [47]. In case of larger number of disruptions, immediate component replacement may occur, earlier than otherwise scheduled. During the disruption, sudden loss of plasma confinement occurs, namely, whole plasma thermal energy is deposited on PFCs. Due to significant heat loads, tungsten-based materials were chosen to achieve the required lifetime – pure tungsten as well as tungsten alloys [47].

The loss of coolant accident (LOCA) is another major issue to the reactor operation and safety. Occurrence of LOCA will lead to reaction termination (often followed by disruption), require reactor shutdown and in worst-case scenario lead to radiation leak outside the reactor. Due to the neutron irradiation, the mechanical and thermal properties of tungsten e.g. ductility and thermal conductivity may degrade during the operation. In addition, tungsten will become neutron activated. Because of the degraded material properties, cracks may occur on tungsten surface and propagate inside, towards the copper or copper alloy (e.g. CuCrZr) cooling channel. Crack propagation may be accelerated, or sudden rupture may occur because of significant thermal shock and electromagnetic force during the disruption [48]. As a result, cooling water ingress in the reactor will occur and temperature will increase significantly. In a similar way, however less likely scenario, structural integrity of vacuum vessel can be disrupted, and internal components can be exposed to outer environment. According to [49], temperature of first wall components will rise promptly and, depending on the reactor/blanket concept, would stay between 800 °C to 1200 °C for up to 100 days.

The calculations were performed without considering active safety systems or operator actions; however conservatively. Therefore, the actual period of high temperatures may be different, nevertheless is likely to be rather longer. Exposed to such conditions, i.e. high temperature, water vapour and outer atmosphere, tungsten will oxidize rapidly. Tungsten oxide is volatile and through the evaporation, radioactivity can be spread to the surrounding environment. In the accidental temperature range, oxidation rate of pure tungsten thin coatings was found to be of the order of 10^{-2} mg/(cm^2·s) [50]. This accounts for about 500 kg of material per hour released from 1500 m^2 DEMO first wall. Promising way to mitigate the excessive tungsten oxidation is alloying with other oxide forming element. In the accidental conditions, compact and stable oxide layer should be formed on the tungsten alloy armour surface (see Figure 7), minimizing the tungsten oxidation and preventing the radiation contamination. Promising results have been reached for alloying with chromium.

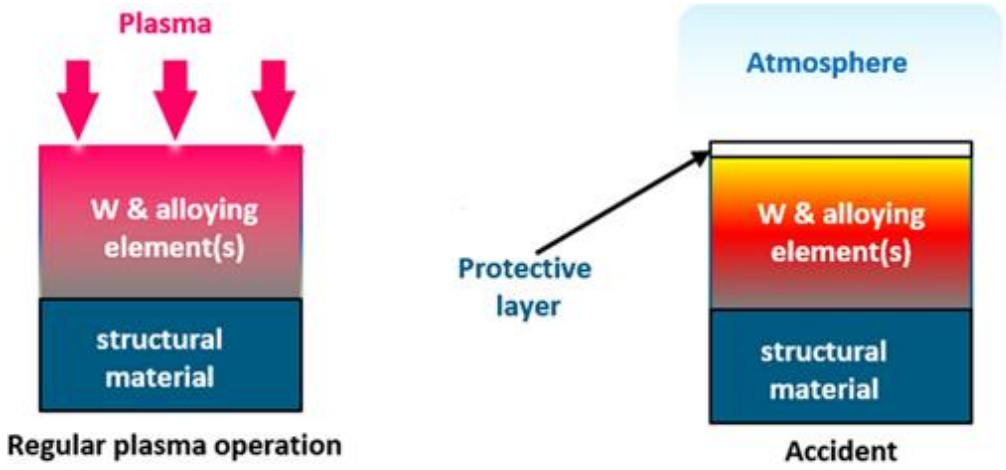

Fig. 7: Scheme of tungsten alloys operation during steady-state (left) and accidental (right) conditions, modified according to [51]. Protective passivating layer (indicated by arrow) is formed after the accident.

5. Materials for Plasma Facing Components

5.1. Pure tungsten as prime candidate for divertor application

Tungsten is a bcc refractory metal. There are several tungsten properties which favour its use in fusion application; the most important are following properties:

- High melting point and good thermal conductivity

  Tungsten has the highest melting point of metals (3410 °C) and good thermal conductivity (155 W/(m·K)). Therefore, tungsten-based materials have the greatest potential to withstand high heat fluxes and temperatures present in the fusion reactor without melting while enabling sufficient heat extraction from the blanket.

- Low hydrogen retention

  As the fuel for the first generation of fusion power plants will be mixture of hydrogen isotopes, all components will be exposed to it. High intake and retention of hydrogen can negatively affect material properties, therefore materials with low hydrogen retention are preferred. In addition, regarding tritium, excessive retention in in-vessel components could cause overshooting of allowable tritium inventory and result in reactor shutdown.

- Low activation

  In-vessel components, mainly PFCs will become activated due to significant neutron fluxes. Therefore, use of low activation elements is preferred. Use of tungsten as PFC material is feasible, as tungsten fulfils the maximum dose rate requirement [52]; however, many elements cannot be used for tungsten alloying due to higher activation (see the Appendix A1). The key quantity is gamma contact dose rate in Sieverts per hour (Sv/h) after 100 years' decay time after irradiation. For hands-on recycling the limit value is 10^{-5} Sv/h, in case of remote handling values up to 10^{-2} Sv/h are acceptable.

- High sputtering resistance

  PCFs will be exposed to significant fluxes of not only neutrons, but other particles as well. Sputtering with ions or neutral atoms could result in material erosion, which could limit the component lifetime. In addition, sputtered atoms may enter the plasma. Radiation losses of heavy elements present in plasma may be so high, that

plasma would be cooled down significantly and fusion reaction would be terminated. These risks should be mitigated in case of tungsten, as sputtering threshold is high.

Through the number of advantages, there are still some issues which must be resolved for pure tungsten, mainly high ductile to brittle transition temperature (DBTT) and low recrystallization temperature. Both temperatures limit the operational space of tungsten components. Below the DBTT material is prone to brittle fracture. This constitutes serious safety threat as the failure occurs suddenly and time to take safety measures is very short. DBTT of the material depends on its purity, microstructure, fabrication route etc. For tungsten, the values usually lie between 300 °C and 700 °C [53]–[55]; however, after recrystallization the DBTT can overcome 1000 °C [56]. Regarding tungsten for PFC application, the DBTT must be below the steady state operation temperature, i.e. ca. 400 °C. In addition, after longer experimental campaign or after venting of the vacuum vessel due to maintenance, amount of adsorbed gas may be too high to reach the required vacuum for plasma operation. Therefore, temperature increase of vacuum vessel and in-vessel components (so-called baking) is required to promote the desorption. For DEMO, the vacuum vessel temperature which allows to perform baking in reasonable time is proposed around 180 °C [57]. Taking into account ITER facility, where the temperature difference between vacuum vessel and blanket/divertor is about 40 °C [34], higher temperature must be expected for DEMO PFCs as well. Although there is no plasma during baking and the thermal stressed are expected to be much lower than during steady state operation, to mitigate any possible risks, DBTT of PFC material should be lowered below the baking temperature, i.e. around 200 °C.

On the other hand, recrystallization temperature sets the upper operational limit. Recrystallization is thermally activated process of formation of new, strain-free grains in the material. Usually the recrystallization is accompanied by reduction in strength and hardness while increasing ductility [58]. For tungsten, significant decrease of fracture toughness [59], yield and ultimate tensile strength was reported [60]. Calculations for ITER divertor showed that surface temperature of tungsten components can easily exceed 1300 °C [61], while

recrystallization can occur already at 1100 °C [62]. Therefore, increase of the recrystallization temperature is necessary.

5.1.1. Optimization of tungsten properties

Experiments aimed on improving ductility by alloying were successful only for few elements, e.g. rhenium [63], iridium or zirconium [64], but the feasibility of these elements is limited by the possible activation or very low abundance (Re, Ir). Therefore, increase of tungsten ductility is usually achieved by applying mechanical deformation during fabrication [65]–[67] e.g. rolling, swaging, high-pressure torsion etc., thus reducing the grain size. Alternatively, fine grain structure and ductility increase can be achieved also by rapid compaction method, e.g. Field Assisted Sintering [68]. However, in case of very fine grains mechanical properties will be governed by the grain boundaries, which may result in brittleness of the material, due to very high number of those boundaries. The grain size must be therefore chosen carefully, to balance these two contradictory tendencies.

Experiments of Tsuchida et al. [62] showed also that recrystallization temperature can be increased by alloying with K and Re, to 1400 °C (K) and 1500 °C (K + Re). This however poses similar difficulties as for DBTT reduction. On the contrary to DBTT, improving of recrystallization temperature was not achieved by larger deformation: the recrystallization onset occurred earlier at given temperature for more deformed samples [69] and recrystallization of heavy deformed tungsten occurred at lower temperature [70] then for less deformed samples [71].

5.2. Tungsten alloys with increased oxidation resistance

For the first wall application where the conditions are not so harsh, compared to the divertor, the mechanical properties of tungsten can be compromised in favour of increasing passive safety. Prevention of tungsten oxidation, i.e. formation of a protective oxide scale on a tungsten alloy, during accidental conditions is the principal issue, as tungsten oxidation can lead to significant radiation contamination (outlined in section 4). To mitigate the consequences of LOCA accident, alloying of tungsten with low activation, oxide forming

element was suggested. Further requirements for the alloying elements are high melting point and good thermal conductivity to avoid the degradation of high-temperature performance of tungsten. Research on increasing oxidation resistance of tungsten began by alloying with silicon, which was later accompanied with chromium [72]. W-Si-Cr alloy showed reduction of oxidation rate at 1000 °C by 4 orders of magnitude. However, later research pointed out possibility of brittle intermetallic formation, which underlined the need for silicon-free alloys. Promising results were reached for W-Cr-Ti system, which exhibited even lower oxidation rate [73]. However, high tritium retention in titanium [74] may compromise fusion power plant operation and therefore, titanium should be omitted from use in PFCs. Nevertheless, alloys of only W and Cr are capable of significant oxide resistance improvement, especially when single solid solution is reached - 5 orders of magnitude lower oxidation rate, compared to pure W [75][76]. Other beneficiary properties can be introduced by alloying with Hf or Y, e.g. grain refinement, improvement of the layer adherence, reduction of oxide layer growth rate and suppressing void formation at oxide-alloy interface [77]. Experiments with W-10.3Cr and W-10.4Cr-1.2Y (wt. %) alloys showed that alloying with yttrium reduced the oxidation rates by at least one order of magnitude. Also, transition from slow to fast oxidation was retarded significantly [75].

5.2.1. Phase stability of W-Cr alloys

To reach the passivation properties, formation of single solid solution of W and Cr is highly desirable. This constitutes major problem, as the W-Cr phase diagram is characterized by a large miscibility gap, see Figure 8. This means that for every composition there is certain temperature, so called critical solution temperature, below which the miscibility of elements is limited. At lower temperatures W-rich and Cr-rich phases are formed, instead of single-phase solid solution, which degrades the oxidation resistance of alloy. Also, mechanical properties can be affected by misfit strains and thermal stresses [78]. Material decomposes at all temperatures below the critical temperature, as solid solution is inherently unstable; however, the kinetics is temperature-dependent and can differ significantly. As mentioned in section 3.2., temperature at the first wall, where tungsten-chromium alloys will be located, during steady-state operation remains deep below the critical temperature. Therefore, kinetics at these temperatures is expected to be very slow, so that the material survives for the whole component lifetime, i.e. several years. During transient events, temperature rise and can get close to or exceed the critical solution temperature. To avoid significant decomposition, sufficient cooling must be employed so that the temperature is quickly lowered to area of slow kinetics. During accidental conditions, temperatures up to 1200 °C are expected, as mentioned in section 4. As the cooling systems will be out of order, the kinetics must be optimized as well, to allow sufficient lifetime until passivation layer formation or accident mitigation, i.e. up to several months. Therefore, optimization of decomposition kinetics is essential in temperature range up to 1200 °C. Respective temperatures are displayed also in Figure 8. The oxidation test on W-Cr alloy have most frequently duration no more than 10h. Within this period effects of decomposition might not be apparent. However, the accidental conditions are expected to take about 100 days or longer before the temperature decreases to the accessible levels [49].

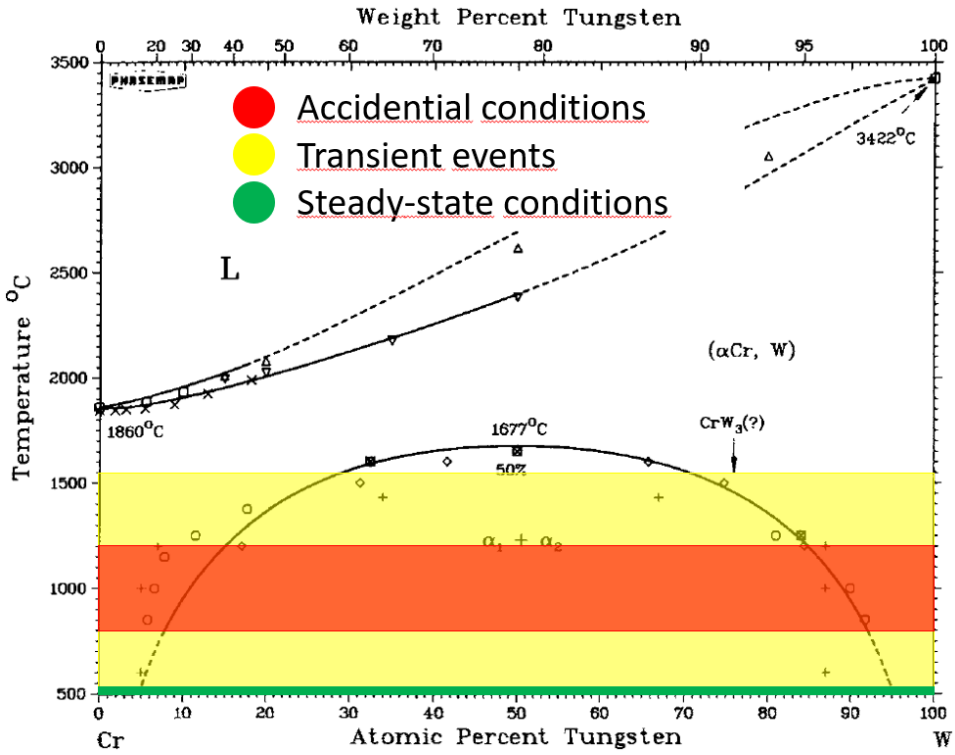

Fig. 8: Phase diagram of W-Cr system, featuring relevant operational temperature ranges of first wall, modified according to [79]. During steady-state operation temperature remains below 500 °C.

Due to the miscibility gap, fabrication of solid solution-based W-Cr alloys is also challenging. Main requirement for the chosen process is sufficiently fast cooling to prevent the decomposition, as the decomposition has certain kinetics [80]. Field Assisted Sintering Technique [81] can serve as an example of a method capable of preserving the solid solution, because of high heating and cooling rates achievable.

6. Powder metallurgy processing of tungsten and tungsten alloys

6.1. Mechanical alloying

Mechanical alloying is a non-equilibrium powder production method, based on breaking the coarse materials to finer compositions and solid-state reactions between the reactant powders. It is usually performed in cylindrical vessel containing powder and balls, able to move freely inside. By colliding with the powder particles, the balls lower the particle size. Original purpose of mechanical alloying was to reduce the powder particle size and to blend the powders. Nowadays, mechanical alloying has become important method of producing broad range of materials, such as

- ODS materials,
- Supersaturated materials,
- Nanomaterials,
- Alloys containing various immiscible metals.

Some of these materials can be prepared by conventional methods as well; however, by using mechanical alloying fabrication can be simplified and unique properties can be introduced [82]. Planetary ball mills are the most common mill type used for alloying. For this type of mills, both the supporting discs and vials filled with powder and balls move autonomously, in opposite directions. Therefore, the centrifugal forces are synchronized and opposite, resulting in the characteristic movement of the balls inside of the vials. Both powders and balls are rolling along the one wall of the vial until reaching a critical point, where they are lifted and thrown on the other side, as can be seen in Figure 9.

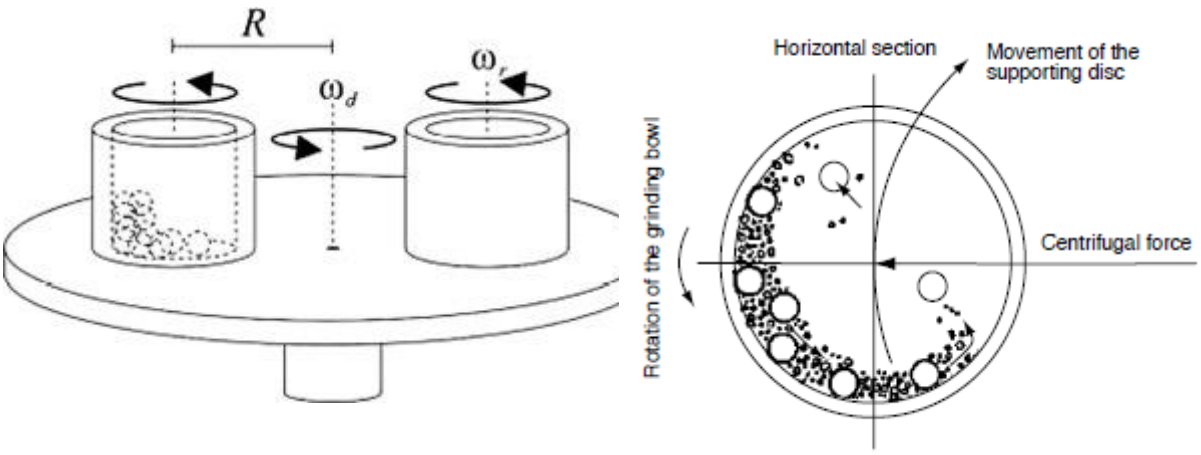

Fig. 9: Scheme of the planetary ball milling principle (left) [83] and movement of the milling balls inside the vials (right) [84].

During the flight, the balls reach high speed, as the effective centrifugal force can reach up to 20 times gravitational acceleration, depending on the rotational speed. Some manufacturers claim to offer devices operating up to 1100 RPM, increasing the forces up to 95 times gravitational acceleration. Vials and milling balls are manufactured from various materials, e.g. steel, tungsten carbide, zirconium oxide etc. and in various sizes, depending on the purpose. Special type of vials also allows to perform the milling in inert or reactive atmosphere, flushing the inside of the vial with the respective gas. Also, double-walled vials with the cooling ability can be used, as significant heat can be generated during the milling process.

Dominant processes during the mechanical alloying are repeated welding, fracturing and re-welding of the powders, as schematically showed in the Figure 10, left. For successful alloying, the balance between welding and fracturing is essential. During the ball-powder-ball collisions, the powder particles are flattened and heavily mechanically deformed, forming layered structure and increasing number of dislocations. Further milling results in microstructure refining, fracturing into smaller particles and interdiffusion reactions promoted by high dislocation density, forming an alloy [85]. This is also described in detail in Figure 10.

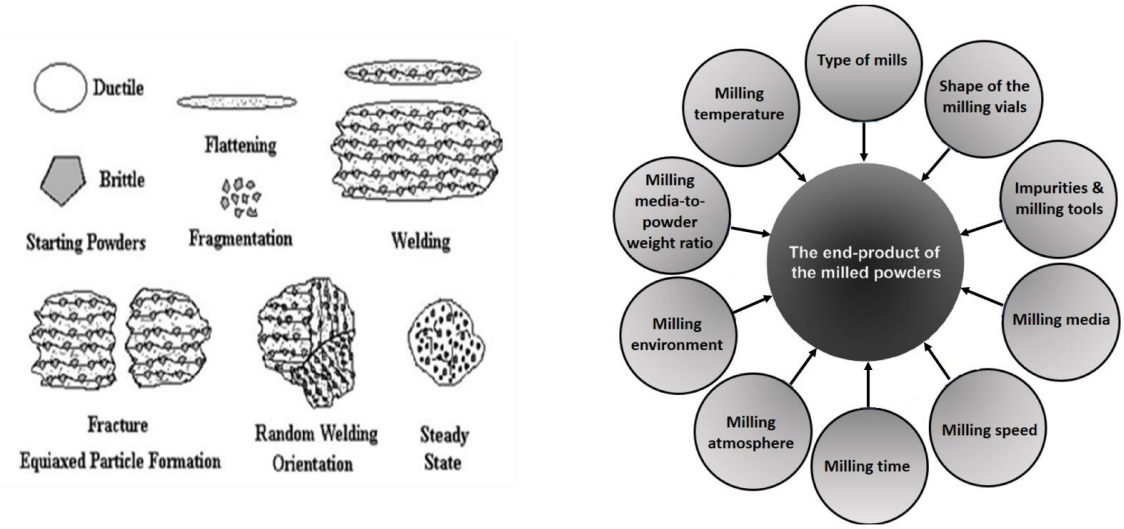

Fig. 10: Different stages of mechanical alloying (left, [86]), main factors affecting the MA process (right, modified according to [87]).

Process of mechanical alloying naturally depends on numerous factors, such as type of the mill, milling speed, milling time etc. Careful choice and control of the processing parameters are essential to obtain the desired final products properties, such as particle size distribution, stoichiometry, degree of alloying etc. Common factors influencing the result of mechanical alloying are presented in Figure 10, right.

6.2. Powder consolidation

Consolidation of the powder into final solid specimen is the second phase of powder metallurgy process. Usually it consists from two subsequent phases – pressing and sintering. During a typical process, certain amount of powder is introduced into a die with the shape of the final product, sealed with the punches and the desired load is applied. The load can be in the range of several tens of MPa up to 1 GPa, with as slow loading rate as possible, to avoid formation of traps and voids. The sample is kept at the certain final load for selected time, from several minutes to hours, to improve the density. However, the final density is about 80-95 % and the product is referred to as a "green compact". The sintering process is then applied on the green compacts to further increase the density, up to values over 99.5 %. The sintering can be pressure-less or pressure-assisted, with the applied temperature of usually 0.7-0.9 T_m (melting temperature) and time from few minutes to several hours. However, for the

consolidation of ball-milled or alloyed powders the conventional methods are often not suitable, due to the long-term subjecting to high temperature. During the sintering step, significant grain coarsening and growth occurs, along with other changes of properties, reached during demanding mechanical alloying process, e.g. amorphous, composite or solid solution microstructure. For such materials, different approaches are suitable, such as cold-isostatic pressing, microwave sintering or field assisted sintering technique (FAST).

6.2.1. Field assisted sintering technique

Field assisted sintering technique is an attractive method of powder consolidation, especially for materials sensitive to temperature or grain growth e.g. nanocrystalline, amorphous or metallic glassy materials. Consolidation can be achieved at lower temperatures and within shorter periods of time due to the simultaneous application of pressure and electric current, pressing and heating the powder. Scheme featuring all characteristic components of FAST equipment can be seen in the Figure 11.

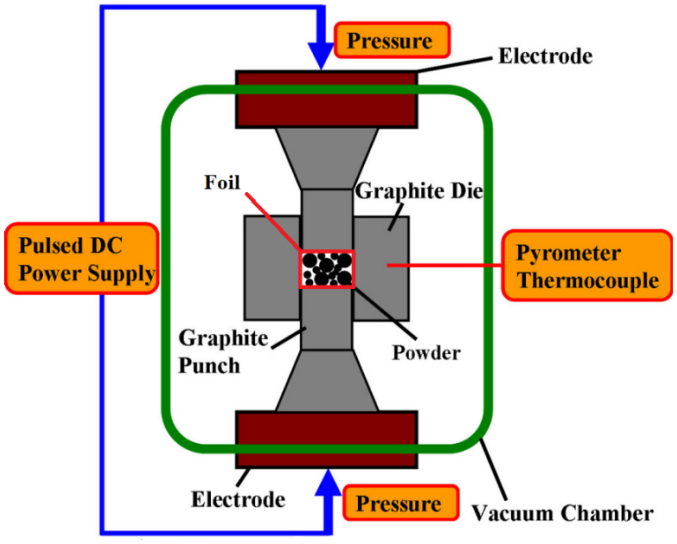

Fig. 11: Field assisted sintering technique, principle and all the essential components, modified according to [88].

Similarly, to conventional sintering, the powder is inserted into the die and placed between punches. The punches are however connected to the electrodes. The die and punches are usually from graphite and to ensure easy ejection, graphite sheets are used as spacers between the powder and all other components. Additional foils from different materials can

be used as a diffusion barrier, as at higher temperatures, diffusion of carbon from the die and punches becomes significant. During the compaction, high pressure and pulsed electric current is applied through the punches. The heating is therefore internal, caused by the passage of electric current (Joule heat), and because of this, very high heating and cooling rates are achievable, up to 2000 °C/min. The applied pressure can be up to 1000 MPa, depending on the material of the punches, usually values of 50-100 MPa are used [89].

7. Aims of the thesis

Ultimate milestone of the thesis was to identify suitable alloying element to prolong the W-Cr solid solution lifetime and successfully prepare the bulk alloy by Field Assisted Sintering. Given that this is rather complex task, the progress was broken down to several minor milestones, each contributing to the overall goal. Essential issues were especially:

- Achieving the desired phase composition of the starting powder
- Preserving the desired composition through the compaction by FAST

Fulfilling these steps was a vital requirement to start the attempts to evaluate and improve the solid solution stability. Considering the time-consuming preparation of the powder material and the subsequent long-term experiments, additional step was added, i.e. computer simulations provided by partners from IT4Innovations (VŠB – Technická univerzita Ostrava), aiming to increase the effectivity of the experiments. The follow-up research was mainly focused on:

- Increasing the W-Cr solid solution lifetime by further minor alloying
- Experimental verification and collaboration in a development of computational software, capable of energy-balance assessment, identifying prospective alloying elements (computer modelling performed by the partners from IT4Innovations)

8. Collection of the articles

Experimental part of the thesis is presented as a collection of articles published in impacted international journals. The papers are ordered chronologically according to the development of the knowledge collected during our research on the stability of W-Cr alloy properties at high temperatures. The first paper deals with sintering of pure tungsten as it is the main element of the alloys tailored within the thesis. The following articles are focused on understanding the phase stability of tungsten-chromium alloys during various thermal treatments.

The first article titled “Evolution of carbon and oxygen concentration in tungsten prepared by field assisted sintering and its effect on ductility” is focused on levels of crucial tungsten impurities – carbon and oxygen [90]. These elements degrade not only mechanical properties of tungsten but also oxidation properties of the tungsten alloys. Experiments were focused on effect of the main sintering process parameters, excluding temperature, on the mechanical properties, microstructure and impurity levels. The main outcome of this study was of a practical character: we understood the mechanism of carbon intake and oxygen reduction during the high temperature sintering of tungsten based materials and identified the most suitable parameters for optimum mechanical properties. This knowledge provided convenient background during consolidation studies of W-Cr alloys.

Initial experiments with sintering of W-Cr alloys resulted in compacts with low porosity, however the alloys experienced undesirable phase changes compared to the original mechanically alloyed powder. This led to depletion of chromium, that is the key component assuring proper oxidation behaviour, from the W-Cr single solid solution, affecting up to half of the final sample thickness. The second article titled “Controlling the carbide formation and chromium depletion in W-Cr alloy during field assisted sintering” explains the mechanisms behind the phase changes and reveals the strategy for the Cr depletion mitigation [81].

In the third article titled “Ultrafine-grained W-Cr composite prepared by controlled W-Cr solid solution decomposition” the knowledge gained on the W-Cr solid solution decomposition was used for tailoring composite materials [91]. The microstructure emerging from the solid solution decomposition has specific morphology features that could enhance the mechanical

performance; therefore, it was decided to examine the basic material properties, microstructural and phase stability of the composites. In addition, the possibility of material properties prediction by computer modelling was explored, as it is very useful and could save significant amount of resources.

In the fourth article titled “Decreasing the W-Cr solid solution decomposition rate: theory, modelling and experimental verification”, the possibility to enhance the stability of W-Cr solid solution by additional alloying was assessed [92]. Computational model was developed to determine prospective alloying elements without trial-and-error approach, thus saving time and resources. Tantalum was identified as a suitable candidate material and annealing experiments confirmed the model predictions, i.e. the prolonged solid solution lifetime. Further extensive XRD experiments provided enough data to characterize the phase evolution and suggest the key rate controlling factors of the decomposition. The results constitute an important achievement in order to extend the W-Cr alloy stability to fusion relevant temperatures.

8.1. Evolution of carbon and oxygen concentration in tungsten prepared by field assisted sintering and its effect on ductility

Tungsten is a refractory metal routinely chosen for wide range of high-temperature applications, including potential application in the nuclear fusion. Due to its very high melting point, fabrication usually involves powder metallurgy methods, either conventional sintering or other sintering methods, e.g. field assisted sintering, flash sintering etc. Although mechanical properties are not the primary concern regarding the use of tungsten in fusion power plants, certain level of some properties must be reached, to ensure reliable and safe operation. One of the most important and most researched properties is ductility of tungsten, which is poor at room temperature and becomes significant only at high temperatures. It is well known that ductility is affected by both microstructural features and impurities present in the material. As the conventional fabrication process of tungsten components is usually very lengthy, the microstructure is coarse-grained leading to poor mechanical properties, including ductility. This can be improved by post-processing, facilitating severe plastic deformation – hammering, rolling etc. – but these are lengthy and expensive. Advanced sintering methods, e.g. field assisted sintering, can achieve significantly faster compaction, therefore the resulting microstructure can be much more favourable. However, the resulting properties are still far from the thermo-mechanically post-processed material. Therefore, to achieve the best possible properties, impurity control is an important strategy during the sintering process. The concerns are related especially to carbon and oxygen, which are known to affect mechanical properties significantly. Certain oxygen level is always present in the starting powder and it is not common to perform whole fabrication under protective atmosphere so oxygen contamination is hard to avoid. Situation with carbon is complicated as well, as most sintering methods use graphite tools for its good conductivity, both thermal and electrical, and high temperature strength. Therefore, significant carbon diffusion can occur during fabrication, especially at higher temperatures. Nevertheless, sintering experiments reported in this paper showed that by using proper process parameters and equipment, it is possible to control the impurities level and to achieve ductility at moderate temperatures without the need for any post-processing.

8.2. Controlling the carbide formation and chromium depletion in W-Cr alloy during field assisted sintering

The second article focuses on quality issues during sintering of alloy based on W-Cr solid solution. It is well known that the phase diagram of tungsten and chromium features a miscibility gap, stretching almost through the whole concentration range. Single solid solution is thus unstable below certain temperature, ranging ca. from 500 °C (for Cr – 15 wt. % or W – 2 wt. % Cr alloy) up to ca. 1700 °C (for W – 20 wt. % Cr alloy), and decomposes into mixture of two different solid solutions. This has detrimental effect on the expected use of W-Cr alloys, where the single solid solution is crucial for expected passivation properties. Nevertheless, as this process is thermally activated there is different kinetics of this phase transformation at different temperature. As it was observed for W – 10 wt. % Cr alloy, where the miscibility gap ends at ca. 1500 °C, the decomposition proceeds very fast at 1200 °C, moderately at 1000 °C and extremely slow at 700 °C. As the traditional method of alloying by melting is not applicable, non-equilibrium room-temperature process of mechanical alloying can be used conveniently. By applying mechanical deformation, solid solution can be prepared, though it is thermodynamically unstable phase. For the compaction, one must use elevated temperature, which is in case of tungsten-chromium usually above the miscibility gap border, thus when a method with sufficiently fast heating and cooling rate is employed, inertia of the process supresses phase transformation. Field assisted sintering fulfils all the requirements, therefore it is possible to routinely produce W-Cr alloy samples featuring single solid solution. However, during sintering in classical setup, i.e. using graphite die, punches and lining foil, an issue with the carbon contamination and a solid solution de-alloying occurred. In addition, the affected depth was significantly bigger than it was expected due to plain diffusion. By changing the processing parameters, the contamination and de-alloying were mitigated. Additional thermogravimetry experiments identified the reasons for such major contamination and enlightened the mitigation mechanism.

8.3. Ultrafine-grained W-Cr composite prepared by controlled W-Cr solid solution decomposition

In the previous study it was observed that by using suitable setup, compact W-Cr alloy samples can be produced by spark plasma sintering, preserving the solid solution achieved previously by mechanical alloying. This study deals with the possibility to tailor the microstructure of alloys derived from W-Cr solid solution. Due to the miscibility gap in W-Cr phase diagram the solid solution is unstable and at higher temperatures tends to decompose. Kinetics of this decomposition at 1000 °C is convenient and allows to produce UFG material featuring fine W-rich and Cr-rich phase (compared to the original composition). Further investigations revealed that such microstructure greatly improved mechanical properties of the material. Samples annealed for 15 hours exhibited up to 65 % higher flexural strength, while the hardness was decreased by 10 %. Elastic properties of the composite material and the original single solid solution are comparable, as confirmed both by experiment and computer modelling. In addition, elastic properties of both new phases, emerging during the decomposition, are calculated as well. Majority of the lamellae that make up the decomposed microstructure is below 200 nm, which is hardly achievable by direct fabrication. The stability of the decomposed microstructure is confirmed by long-term annealing at 700 °C, which corresponds with the stability of as-sintered samples [80]. Computational modelling proved to be viable tool for predicting elastic properties even of alloys with complex phase diagrams and submicron microstructure.

8.4. Decreasing the W-Cr solid solution decomposition rate: theory, modelling and experimental verification

After stabilizing the microstructure of W-Cr alloy, the fourth article focuses on enhancing the single phase lifetime by additional alloying. In order to avoid time-consuming and costly experiments, computer modelling was employed to assess the thermodynamics of the W-Cr system. Number of possible alloying elements was reduced to fulfil the material design restrictions for fusion environment, and tantalum was chosen as the most promising alternative. Based on these results, W - 10 wt. % Cr - 2 wt. % Ta alloy was successfully produced by MA and FAST, and annealing experiments were performed. The results confirmed the theoretical predictions, as the decomposition rate of solid solution was decreased significantly. SEM, EDS and XRD investigation then identified the key mechanisms of the decomposition retardation. High affinity of Ta to Cr results in Ta incorporation into the Cr-rich phase which originates at the grain boundaries during the decomposition. At the early stages of transformation, the Ta content is higher than the equilibrium values. The excess Ta is then transported by the diffusion, retarding further formation of decomposed phase. Especially for short annealing times, the decomposition is significantly slowed down. During long-term annealing, diffusion of Ta results in formation of whole new phase with high lattice parameter. This phase was identified as a mixed W-Cr-Ta bcc phase, with very small crystallite size. Developed computer model was capable to accurately predict the effect of tantalum on the alloy stability. In addition, effect of hafnium was examined and the results of the model corresponded well to the previous findings. Relative change of both W-Cr-Hf and W-Cr-Ta alloys´ decomposition kinetics acquired from the experiments, was of the same order of magnitude as the one predicted from the first-principles calculations, when compared to the original W-Cr solid solution.

9. Conclusions

Over the course of compiling this thesis, nuclear fusion research surpassed several milestones, so far reaching about 80% completion of the ITER facility. Multiple DEMO reactor design studies and design studies of the auxiliary facilities have also been published in many countries. That makes the material engineering of tungsten based alloys highly relevant, as the key issues are not yet satisfactorily resolved. Approach and main results of the journal articles, compiled into this thesis, contribute to deeper understanding of the material design and preparation, with prospective future outlook. Crucial achievement at the beginning of the study was the identification of the parameters and setup ensuring samples with the right phase composition and low level of impurities. It was observed that although the FAST environment is inherently oxide-reducing and carburizing, the resulting impurity levels can differ significantly. Apart from the intuitive time dependence, i.e. decreasing oxygen content and increasing carbon content with increasing sintering time, atmosphere present within the experimental chamber has a serious impact on the results. Regarding this, sintering in vacuum yielded the best results, while using hydrogen-containing atmosphere was less effective. The oxide-reducing ability was comparable with the other environments, while the carbon content was significantly higher. As the most viable theory, it was adopted that during the sintering, hydrocarbon gas may form and therefore the contamination can spread faster and deeper into the sample. The effect was more pronounced when additional tungsten protective foil was used, due to sample overheating. The use of tungsten foil, however, was necessary for W-Cr alloys. It was observed that presence of chromium lowers the melting point of tungsten carbide and results in liquid sintering, further increasing the contaminated area. The tungsten foil has postponed the direct contact of chromium and carbon, consequently leading to significant reduction of carbon contamination and preventing de-alloying of the W-Cr solid solution alloy. With the production process optimized, stability of the W-Cr solid solution could be investigated. It was confirmed that at 1000 °C the decomposition proceeds fast, however; at 700 °C the alloy exhibits very good long-term stability. With the prospect of preparing homogeneous fine grained material, stability assessment was performed also on

the decomposed samples. It was observed that at 700 °C the decomposition does not proceed further and therefore annealing can be used to prepare stable UFG W-Cr composite material. Subsequent mechanical testing proved that there is significant improvement in both room- and high-temperature strength without increase in hardness or change in elastic properties. Computational model was also developed and proved to be useful tool to determine the alloy elastic properties, even of the individual phases, which are impossible to be measured conventionally. In light of these findings, further alloying was attempted, to prolong the solid solution stability. The developed model was modified to help determining the suitable element, from the range of elements allowed in fusion-reactor environment. Based on the results, alloying with tantalum was proposed and successfully performed. Decomposition kinetics was slowed down significantly, yielding up to four times longer lifetime. During the experiments, complex interaction of Cr with Ta was identified and explained, presumably responsible for the stability improvement. These results confirmed alloying as a promising way to stabilize the single solid solution. In addition, *ab-initio* calculations proved to be viable tool to limit costly trial-and-error approach and to make the workflow smoother and more effective.

References

[1] I. E. Agency, “World Development Indicators (WDI) | Data Catalog.” [Online]. Available: http://data.worldbank.org/data-catalog/world-development-indicators. [Accessed: 20-May-2020].

[2] G. McCracken and P. Stott, “Why We Will Need Fusion Energy,” in *Fusion*, Elsevier, 2013, pp. 189–202.

[3] “World Energy Outlook 2017 – Analysis - IEA.” [Online]. Available: https://www.iea.org/reports/world-energy-outlook-2017. [Accessed: 14-May-2020].

[4] C. Quéré *et al.*, “Global Carbon Budget 2018,” *Earth Syst. Sci. Data*, vol. 10, no. 4, pp. 2141–2194, Dec. 2018.

[5] D. Gilfillan, G. Marland, T. Boden, and R. Andres, “Global, Regional and National Fossil-Fuel CO2 Emissions,” 2019. [Online]. Available: https://energy.appstate.edu/CDIAC. [Accessed: 18-May-2020].

[6] D. Hoegh-Guldberg, O. *et al.*, “Global Warming of 1.5 ^{o}C,” pp. 177–287, 2014.

[7] R. W. Wimbadi and R. Djalante, “From decarbonization to low carbon development and transition: A systematic literature review of the conceptualization of moving toward net-zero carbon dioxide emission (1995–2019),” *Journal of Cleaner Production*, vol. 256. Elsevier Ltd, p. 120307, 20-May-2020.

[8] V. Masson-Delmotte *et al.*, “IPCC, 2021: Summary for Policymakers,” *Clim. Chang. 2021 Phys. Sci. Basis. Contrib. Work. Gr. I to Sixth Assess. Rep. Intergov. Panel Clim. Chang.*, 2021.

[9] “WMO LC Annual-to-Decadal Climate Prediction.” [Online]. Available: https://hadleyserver.metoffice.gov.uk/wmolc/. [Accessed: 22-Sep-2021].

[10] B. W. Brook, A. Alonso, D. A. Meneley, J. Misak, T. Blees, and J. B. van Erp, “Why nuclear energy is sustainable and has to be part of the energy mix,” *Sustain. Mater. Technol.*, vol. 1, pp. 8–16, Dec. 2014.

[11] C. L. Chiu and T. H. Chang, “What proportion of renewable energy supplies is needed to initially mitigate CO2 emissions in OECD member countries?,” *Renewable and Sustainable Energy Reviews*, vol. 13, no. 6–7. Pergamon, pp. 1669–1674, 01-Aug-2009.

[12] Nuclear Energy Agency and International Atomic Energy Agency, *Uranium 2016*. France: OECD Publishing, 2016.

[13] H. D. Lightfoot, W. Manheimer, D. A. Meneley, D. Pendergast, and G. S. Stanford, “Nuclear fission fuel is inexhaustible,” in *2006 IEEE EIC Climate Change Technology Conference, EICCCC 2006*, 2006.

[14] A. Gabbard, “Coal combustion: nuclear resource or danger,” *Oak Ridge Natl. Lab. Rev.*, 1993.

[15] J. D. Lawson, “Some criteria for a power producing thermonuclear reactor,” *Proc. Phys. Soc. Sect. B*, vol. 70, no. 1, pp. 6–10, 1957.

[16] A. C. (Anthony C. . Phillips, *The physics of stars*. John Wiley, 1999.

[17] “Advantages of Fusion,” *ITER Organization*, 2019. [Online]. Available: https://www.iter.org/sci/Fusion. [Accessed: 30-Mar-2020].

[18] J. H. You *et al.*, “European DEMO divertor target: Operational requirements and material-design interface,” *Nucl. Mater. Energy*, vol. 9, pp. 171–176, Dec. 2016.

[19] S. Nogami, M. Toyota, W. Guan, A. Hasegawa, and Y. Ueda, “Degradation of tungsten monoblock divertor under cyclic high heat flux loading,” *Fusion Eng. Des.*, vol. 120, pp. 49–60, Jul. 2017.

[20] V. Shah, M. P. F. H. L. van Maris, J. A. W. van Dommelen, and M. G. D. Geers, “Experimental investigation of the microstructural changes of tungsten monoblocks exposed to pulsed high heat loads,” *Nucl. Mater. Energy*, vol. 22, p. 100716, Jan. 2020.

[21] S. Panayotis *et al.*, “Self-castellation of tungsten monoblock under high heat flux loading and impact of material properties,” *Nucl. Mater. Energy*, vol. 12, pp. 200–204, Aug. 2017.

[22] “tokamak_poster.jpg (JPEG obrázek, 3716 × 2718 bodů) - Měřítko (39%).” [Online]. Available: https://www.iter.org/doc/www/content/com/Lists/Mag Stories/Attachments/65/tokamak_poster.jpg. [Accessed: 19-Feb-2020].

[23] M. R. Gilbert, S. L. Dudarev, D. Nguyen-Manh, S. Zheng, L. W. Packer, and J. C. Sublet, “Neutron-induced dpa, transmutations, gas production, and helium embrittlement of fusion materials,” *J. Nucl. Mater.*, vol. 442, no. 1-3 SUPPL.1, pp. S755–S760, Nov. 2013.

[24] E. Wakai *et al.*, “Radiation hardening and -embrittlement due to He production in F82H steel irradiated at 250 °c in JMTR,” in *Journal of Nuclear Materials*, 2005, vol. 343, no. 1–3, pp. 285–296.

[25] D. Terentyev, M. Vilémová, C. Yin, J. Veverka, A. Dubinko, and J. Matějíček, “Assessment of mechanical properties of SPS-produced tungsten including effect of neutron irradiation,” *Int. J. Refract. Met. Hard Mater.*, vol. 89, p. 105207, Jun. 2020.

[26] S. Cui *et al.*, “Thermal conductivity reduction of tungsten plasma facing material due to helium plasma irradiation in PISCES using the improved 3-omega method,” *J. Nucl. Mater.*, vol. 486, pp. 267–273, Apr. 2017.

[27] M. Beckers, W. Biel, M. Tokar, and U. Samm, “Investigations of the first-wall erosion of DEMO with the CELLSOR code,” *Nucl. Mater. Energy*, vol. 12, pp. 1163–1170, Aug. 2017.

[28] I. [Hrsg. . Pleli, “Nuclear Fusion Programme: Annual Report of the Association Karlsruhe Institute of Technology/EURATOM ; January 2012 - December 2012 (KIT Scientific Reports ; 7647),” 2013.

[29] L. El-Guebaly, P. Wilson, M. Sawan, D. Henderson, and A. Varuttamaseni, “Recycling issues facing target and RTL materials of inertial fusion designs,” in *Nuclear Instruments and Methods in Physics Research, Section A: Accelerators, Spectrometers, Detectors and Associated Equipment*, 2005, vol. 544, no. 1–2, pp. 104–110.

[30] T. Depover, D. Pérez Escobar, E. Wallaert, Z. Zermout, and K. Verbeken, “Effect of hydrogen charging on the mechanical properties of advanced high strength steels,” *Int. J. Hydrogen Energy*, vol. 39, no. 9, pp. 4647–4656, Mar. 2014.

[31] Y. Murakami and S. Matsuoka, “Effect of hydrogen on fatigue crack growth of metals,” *Eng. Fract. Mech.*, vol. 77, no. 11, pp. 1926–1940, Jul. 2010.

[32] C. Quiros *et al.*, “Blistering and hydrogen retention in poly- and single- crystals of aluminum by a joint experimental-modeling approach,” *Nucl. Mater. Energy*, vol. 20, p. 100675, Aug. 2019.

[33] M. Nishi, T. Yamanishi, and T. Hayashi, “Study on tritium accountancy in fusion DEMO plant at JAERI,” in *Fusion Engineering and Design*, 2006, vol. 81 A, no. 1–4, pp. 745–751.

[34] “ITER Technical Basis | IAEA,” *ITER IAEA EDA Documentation Series, No 24, IAEA, Vienna, 2002.* [Online]. Available: https://www.iaea.org/publications/6492/iter-technical-basis. [Accessed: 05-Feb-2020].

[35] “Structural materials for DEMO: Develeopment, Testing and Modelling, R. Lässer et al., 24th SOFT, 11-15 Sept. 2006, Warsaw.”

[36] L. Giancarli, J. P. Bonal, A. Li Puma, B. Michel, P. Sardain, and J. F. Salavy, “Conceptual design of a high temperature water-cooled divertor for a fusion power reactor,” *Fusion Eng. Des.*, vol. 75–79, no. SUPPL., pp. 383–386, Nov. 2005.

[37] H. Greuner *et al.*, “Progress in high heat flux testing of European DEMO divertor mock-ups,” *Fusion Eng. Des.*, vol. 146, pp. 216–219, Sep. 2018.

[38] R. Fetzer, Y. Igitkhanov, and B. Bazylev, “Efficiency of water coolant for DEMO divertor,” *Fusion Eng. Des.*, vol. 98–99, pp. 1290–1293, Oct. 2015.

[39] S. J. Zinkle and J. T. Busby, “Structural materials for fission & fusion energy,” *Materials Today*, vol. 12, no. 11. Elsevier, pp. 12–19, 01-Nov-2009.

[40] T. R. Barrett *et al.*, “Progress in the engineering design and assessment of the European DEMO first wall and divertor plasma facing components,” *Fusion Eng. Des.*, vol. 109–111, pp. 917–924, Nov. 2016.

[41] V. Barabash, K. Ioki, M. Merola, G. Sannazzaro, and N. Taylor, “Materials for the ITER vacuum vessel and in-vessel components – current status, First Joint ITER-IAEA Technical Meeting on ‘Analysis of ITER Materials and Technologies,’” 2010.

[42] C. Bachmann *et al.*, “Key design integration issues addressed in the EU DEMO pre-concept design phase,” *Fusion Eng. Des.*, vol. 156, p. 111595, Jul. 2020.

[43] K. Jiang, E. Martelli, P. Agostini, S. Liu, and A. Del Nevo, “Investigation on cooling performance of WCLL breeding blanket first wall for EU DEMO,” *Fusion Eng. Des.*, vol. 146, pp. 2748–2756, Sep. 2019.

[44] E. Martelli, G. Caruso, F. Giannetti, and A. Del Nevo, “Thermo-hydraulic analysis of EU DEMO WCLL breeding blanket,” *Fusion Eng. Des.*, vol. 130, pp. 48–55, May 2018.

[45] F. Maviglia *et al.*, “Impact of plasma thermal transients on the design of the EU DEMO first wall protection,” *Fusion Eng. Des.*, vol. 158, p. 111713, Sep. 2020.

[46] M. Merola *et al.*, “ITER plasma-facing components,” *Fusion Eng. Des.*, vol. 85, no. 10–12, pp. 2312–2322, Dec. 2010.

[47] C. E. Kessel *et al.*, “Overview of the fusion nuclear science facility, a credible break-in step on

the path to fusion energy," *Fusion Eng. Des.*, vol. 135, pp. 236–270, Oct. 2018.

[48] T. Hino, Y. Hirohata, and T. Yamashina, "Analysis for loss of coolant accident in a fusion reactor," *Fusion Eng. Des.*, vol. 31, no. 3, pp. 259–263, Aug. 1996.

[49] D. Maisonnier *et al.*, "The European power plant conceptual study," *Fusion Eng. Des.*, vol. 75–79, no. SUPPL., pp. 1173–1179, Nov. 2005.

[50] F. Koch and H. Bolt, "Self passivating W-based alloys as plasma facing material for nuclear fusion," in *Physica Scripta T*, 2007, vol. T128, pp. 100–105.

[51] A. Litnovsky *et al.*, "Advanced smart tungsten alloys for a future fusion power plant," *Plasma Phys. Control. Fusion*, vol. 59, no. 6, p. 064003, Apr. 2017.

[52] M. R. Gilbert, J.-C. Sublet, and R. A. Forrest, "Handbook of activation, transmutation and radiation dmagae properties of the elements simulated using FISPACT-II and TENDL-2014," 2015.

[53] Y. Zhang, A. V. Ganeev, J. T. Wang, J. Q. Liu, and I. V. Alexandrov, "Observations on the ductile-to-brittle transition in ultrafine-grained tungsten of commercial purity," *Mater. Sci. Eng. A*, vol. 503, no. 1–2, pp. 37–40, Mar. 2009.

[54] S. Nogami, S. Watanabe, J. Reiser, M. Rieth, S. Sickinger, and A. Hasegawa, "Improvement of impact properties of tungsten by potassium doping," *Fusion Eng. Des.*, vol. 140, pp. 48–61, Mar. 2019.

[55] S. Lang *et al.*, "Microstructure, basic thermal–mechanical and Charpy impact properties of W-0.1 wt.% TiC alloy via chemical method," *J. Alloys Compd.*, vol. 660, pp. 184–192, Mar. 2016.

[56] Q. Yan, X. Zhang, T. Wang, C. Yang, and C. Ge, "Effect of hot working process on the mechanical properties of tungsten materials," *J. Nucl. Mater.*, vol. 442, no. 1–3, pp. S233–S236, Nov. 2013.

[57] T. Haertl, C. Bachmann, E. Diegele, and G. Federici, "Rationale for the selection of the operating temperature of the DEMO vacuum vessel," *Fusion Eng. Des.*, vol. 146, pp. 1096–1099, Sep. 2019.

[58] G. Pintsuk, "Tungsten as a plasma-facing material," in *Comprehensive Nuclear Materials*, vol. 4, Elsevier Ltd, 2012, pp. 551–581.

[59] X. X. Zhang, Q. Z. Yan, C. T. Yang, T. N. Wang, M. Xia, and C. C. Ge, "Recrystallization temperature of tungsten with different deformation degrees," *Rare Met.*, vol. 35, no. 7, pp. 566–570, Jul. 2016.

[60] S. Panayotis *et al.*, "Fracture modes of ITER tungsten divertor monoblock under stationary thermal loads," *Fusion Eng. Des.*, vol. 125, pp. 256–262, Dec. 2017.

[61] R. A. Pitts *et al.*, "Physics conclusions in support of ITER W divertor monoblock shaping," *Nucl. Mater. Energy*, vol. 12, pp. 60–74, Aug. 2017.

[62] K. Tsuchida, T. Miyazawa, A. Hasegawa, S. Nogami, and M. Fukuda, "Recrystallization behavior of hot-rolled pure tungsten and its alloy plates during high-temperature annealing," *Nucl. Mater. Energy*, vol. 15, pp. 158–163, May 2018.

[63] G. Geach and J. Hughes, “The Alloys of Rhenium with Molybdenum or With Tungsten and Having Good High Temperature Properties,” in *Plansee Proceedings 1955, Sintered High-temperature and Corrosion-resistant Materials: Papers Presented at the Second Plansee Seminar*, pp. 245–253.

[64] R. Liu *et al.*, “Fabricating high performance tungsten alloys through zirconium micro-alloying and nano-sized yttria dispersion strengthening,” *J. Nucl. Mater.*, vol. 451, no. 1–3, pp. 35–39, Aug. 2014.

[65] M. Faleschini, H. Kreuzer, D. Kiener, and R. Pippan, “Fracture toughness investigations of tungsten alloys and SPD tungsten alloys,” *J. Nucl. Mater.*, vol. 367-370 A, no. SPEC. ISS., pp. 800–805, Aug. 2007.

[66] Q. Wei *et al.*, “Mechanical behavior and dynamic failure of high-strength ultrafine grained tungsten under uniaxial compression,” *Acta Mater.*, vol. 54, no. 1, pp. 77–87, Jan. 2006.

[67] Q. Wei *et al.*, “Microstructure and mechanical properties of super-strong nanocrystalline tungsten processed by high-pressure torsion,” *Acta Mater.*, vol. 54, no. 15, pp. 4079–4089, Sep. 2006.

[68] J. Veverka, M. Vilémová, Z. Chlup, H. Hadraba, and J. Matějíček, “Optimization of processing parameters for improving the stress-strain performance of FAST tungsten,” *Int. J. Refract. Met. Hard Mater.*

[69] U. M. Ciucani, A. Thum, C. Devos, and W. Pantleon, “Recovery and recrystallization kinetics of differently rolled, thin tungsten plates in the temperature range from 1325 °C to 1400 °C,” *Nucl. Mater. Energy*, vol. 20, p. 100701, Aug. 2019.

[70] A. Alfonso, D. Juul Jensen, G. N. Luo, and W. Pantleon, “Thermal stability of a highly-deformed warm-rolled tungsten plate in the temperature range 1100-1250 °c,” *Fusion Eng. Des.*, vol. 98–99, pp. 1924–1928, Oct. 2015.

[71] A. Alfonso, D. Juul Jensen, G. N. Luo, and W. Pantleon, “Recrystallization kinetics of warm-rolled tungsten in the temperature range 1150-1350 °c,” *J. Nucl. Mater.*, vol. 455, no. 1, pp. 591–594, Dec. 2014.

[72] F. Koch and H. Bolt, “Self passivating W-based alloys as plasma facing material for nuclear fusion,” *Phys. Scr.*, vol. 2007, no. T128, 2007.

[73] F. Koch, J. Brinkmann, S. Lindig, T. P. Mishra, and C. Linsmeier, “Oxidation behaviour of silicon-free tungsten alloys for use as the first wall material,” in *Physica Scripta T*, 2011, vol. T145.

[74] K. L. Wilson and A. E. Pontau, “Deuterium trapping and release in titanium-based coatings for TFTR,” *J. Nucl. Mater.*, vol. 93–94, pp. 569–574, Oct. 1980.

[75] T. Wegener *et al.*, “Development of yttrium-containing self-passivating tungsten alloys for future fusion power plants,” *Nucl. Mater. Energy*, vol. 9, pp. 394–398, Dec. 2016.

[76] A. Calvo *et al.*, “Self-passivating tungsten alloys of the system W-Cr-Y for high temperature applications,” *Int. J. Refract. Met. Hard Mater.*, vol. 73, pp. 29–37, Jun. 2018.

[77] D. P. Whittle and J. Stringer, “Improvements in high temperature oxidation resistance by additions of reactive elements or oxide dispersions,” *Philos. Trans. R. Soc. London. Ser. A,*

Math. Phys. Sci., vol. 295, no. 1413, pp. 309–329, Feb. 1980.

[78] A. Calvo *et al.*, "Manufacturing and testing of self-passivating tungsten alloys of different composition," *Nucl. Mater. Energy*, vol. 9, pp. 422–429, Dec. 2016.

[79] S. V. N. Naidu, A. M. Sriramamurthy, and P. R. Rao, "The Cr-W (Chromium-Tungsten) system," *Bull. Alloy Phase Diagrams*, vol. 5, no. 3, pp. 289–292, Jun. 1984.

[80] M. Vilémová, K. Illková, F. Lukáč, J. Matějíček, J. Klečka, and J. Leitner, "Microstructure and phase stability of W-Cr alloy prepared by spark plasma sintering," *Fusion Eng. Des.*, vol. 127, pp. 173–178, Feb. 2018.

[81] M. Vilémová, F. Lukáč, J. Veverka, K. Illková, and J. Matějíček, "Controlling the carbide formation and chromium depletion in W-Cr alloy during field assisted sintering," *Int. J. Refract. Met. Hard Mater.*, vol. 79, pp. 217–223, Feb. 2019.

[82] M. S. El-Eskandarany, "Introduction," in *Mechanical Alloying*, Elsevier, 2015, pp. 1–12.

[83] F. Delogu, G. Gorrasi, and A. Sorrentino, "Fabrication of polymer nanocomposites via ball milling: Present status and future perspectives," *Progress in Materials Science*, vol. 86. Elsevier Ltd, pp. 75–126, 01-May-2017.

[84] V. Baheti, R. Abbasi, and J. Militky, "Ball milling of jute fibre wastes to prepare nanocellulose," *World J. Eng.*, vol. 9, no. 1, pp. 45–50, Mar. 2012.

[85] M. S. El-Eskandarany, "The history and necessity of mechanical alloying," in *Mechanical Alloying*, Elsevier, 2015, pp. 13–47.

[86] M. Abareshi, S. M. Zebarjad, and E. K. Goharshadi, "Study of the morphology and granulometry of polyethylene-clay nanocomposite powders," *J. Vinyl Addit. Technol.*, vol. 16, no. 1, pp. 90–97, Mar. 2010.

[87] M. S. El-Eskandarany, "Controlling the powder milling process," in *Mechanical Alloying*, Elsevier, 2015, pp. 48–83.

[88] A. Chang *et al.*, "Spark Plasma Sintering of Negative Temperature Coefficient Thermistor Ceramics," in *Sintering Techniques of Materials*, InTech, 2015.

[89] M. S. El-Eskandarany, "Ball milling as a powerful nanotechnological tool for fabrication of nanomaterials," in *Mechanical Alloying*, Elsevier, 2015, pp. 84–112.

[90] J. Veverka *et al.*, "Evolution of carbon and oxygen concentration in tungsten prepared by field assisted sintering and its effect on ductility," *Int. J. Refract. Met. Hard Mater.*, vol. 97, p. 105499, Jun. 2021.

[91] J. Veverka *et al.*, "Ultrafine-grained W-Cr composite prepared by controlled W-Cr solid solution decomposition," *Mater. Lett.*, vol. 304, p. 130728, Dec. 2021.

[92] J. Veverka *et al.*, "Decreasing the W-Cr solid solution decomposition rate: Theory, modelling and experimental verification," *J. Nucl. Mater.*, vol. 576, p. 154288, Apr. 2023.

Appendix A1 – activation properties of pure elements

In table A the activation properties of pure elements are presented. The gamma contact dose rate in Sieverts per hour (Sv/h) after 100 years' decay time after irradiation. The irradiation parameters were simulated to match the situation after 2 full power years of DEMO first wall components. Two limit values are set for design assessment – components exhibiting dose rate from 10^{-5} to 10^{-2} Sv/h are safe for remote recycling, while dose rate lower than 10^{-5} Sv/h are safe for hands-on recycling. The table is divided into four columns, according to the resulting dose rate, i.e. suitability for use as first wall material – higher than 10^{-2} Sv/h (red, unsuitable), 10^{-5} to 10^{-2} Sv/h (yellow, suitable for remote handling) and lower than 10^{-5} Sv/h (green, preferred). Elements in the last green column do not get activated at all or recorded dose rate is under detection limit. Data was acquired from [52].

HIGH ACTIVATION		REMOTE HANDLING		HANDS-ON HANDLING		NO ACTIVATION/BELOW DETECTION LIMIT
Eu	$7{,}15\cdot10^{2}$	**Cd**	$3{,}69\cdot10^{-2}$	**Lu**	$8{,}37\cdot10^{-5}$	**H**
Tb	$2{,}30\cdot10^{2}$	**Os**	$3{,}65\cdot10^{-2}$	**Ce**	$6{,}84\cdot10^{-5}$	**He**
Ho	$5{,}56\cdot10^{1}$	**Tm**	$3{,}31\cdot10^{-2}$	**Re**	$6{,}01\cdot10^{-5}$	**Li**
Ag	$2{,}90\cdot10^{1}$	**Al**	$2{,}88\cdot10^{-2}$	**Ta**	$5{,}07\cdot10^{-5}$	**Be**
Nb	$1{,}12\cdot10^{1}$	**Ni**	$1{,}14\cdot10^{-2}$	**Ca**	$2{,}83\cdot10^{-5}$	**B**
Bi	$5{,}39\cdot10^{0}$	**Cu**	$1{,}10\cdot10^{-2}$	**Pb**	$2{,}60\cdot10^{-5}$	**C**
Ir	$4{,}57\cdot10^{0}$	**Kr**	$9{,}83\cdot10^{-3}$	**Br**	$2{,}51\cdot10^{-5}$	**N**
Sm	$2{,}89\cdot10^{0}$	**Cs**	$6{,}29\cdot10^{-3}$	**Zn**	$2{,}12\cdot10^{-5}$	**O**
Co	$1{,}62\cdot10^{0}$	**Sn**	$2{,}35\cdot10^{-3}$	**W**	$1{,}54\cdot10^{-5}$	**F**
Dy	$7{,}96\cdot10^{-1}$	**Rb**	$1{,}80\cdot10^{-3}$	**Yb**	$1{,}42\cdot10^{-5}$	**Ne**
Gd	$6{,}79\cdot10^{-1}$	**Nd**	$1{,}63\cdot10^{-3}$	**K**	$8{,}60\cdot10^{-6}$	

HIGH ACTIVATION		REMOTE HANDLING		HANDS-ON HANDLING		
Xe	$5{,}55 \cdot 10^{-1}$	**Sc**	$5{,}70 \cdot 10^{-4}$	**Hg**	$7{,}20 \cdot 10^{-6}$	
Hf	$3{,}81 \cdot 10^{-1}$	**Ru**	$3{,}66 \cdot 10^{-4}$	**In**	$6{,}84 \cdot 10^{-6}$	
Er	$3{,}78 \cdot 10^{-1}$	**La**	$3{,}24 \cdot 10^{-4}$	**Te**	$6{,}84 \cdot 10^{-6}$	
Pt	$3{,}29 \cdot 10^{-1}$	**Sb**	$3{,}16 \cdot 10^{-4}$	**Si**	$6{,}71 \cdot 10^{-6}$	
Ba	$2{,}44 \cdot 10^{-1}$	**Zr**	$2{,}97 \cdot 10^{-4}$	**Rh**	$4{,}55 \cdot 10^{-6}$	
Pd	$1{,}86 \cdot 10^{-1}$	**Ti**	$1{,}20 \cdot 10^{-4}$	**Cl**	$4{,}54 \cdot 10^{-6}$	
Mo	$1{,}64 \cdot 10^{-1}$	**Sr**	$1{,}07 \cdot 10^{-4}$	**Fe**	$4{,}25 \cdot 10^{-6}$	
				Au	$2{,}43 \cdot 10^{-6}$	
				P	$8{,}67 \cdot 10^{-7}$	
				Ar	$6{,}28 \cdot 10^{-7}$	
				Y	$2{,}45 \cdot 10^{-7}$	
				Pr	$1{,}69 \cdot 10^{-7}$	
				Mn	$6{,}39 \cdot 10^{-8}$	
				Tl	$4{,}90 \cdot 10^{-8}$	
				Mg	$1{,}37 \cdot 10^{-8}$	
				Se	$5{,}96 \cdot 10^{-9}$	
				V	$4{,}32 \cdot 10^{-9}$	
				S	$3{,}02 \cdot 10^{-9}$	
				I	$9{,}59 \cdot 10^{-10}$	
				Na	$1{,}56 \cdot 10^{-10}$	
				Cr	$3{,}11 \cdot 10^{-11}$	
				Ga	$1{,}78 \cdot 10^{-11}$	
				Ge	$7{,}04 \cdot 10^{-12}$	
				As	$1{,}15 \cdot 10^{-18}$	

Tab. A: Gamma contact dose rate 100 years after end of irradiation, equal to conditions in fusion reactor [52].

Appendix A2 – List of author´s publications related to the thesis

[I] VILÉMOVÁ M., LUKÁČ F., VEVERKA J., ILLKOVÁ K., MATĚJÍČEK J.: Controlling the carbide formation and chromium depletion in W-Cr alloy during field assisted sintering. International Journal of Refractory Metals & Hard Materials, 2019.

[II] VEVERKA J., VILÉMOVÁ M., CHLUP Z., HADRABA H., LUKÁČ F., CSÁKI Š., MATĚJÍČEK J., VONTOROVÁ J., CHRÁSKA T.: Evolution of carbon and oxygen concentration in tungsten prepared by field assisted sintering and its effect on ductility. International Journal of Refractory Metals & Hard Materials, 2021.

[III] VEVERKA J., LUKÁČ F., KADZIELAWA A. P., KOLLER M., CHLUP Z., HADRABA H., KARLÍK M., LEGUT D., VONTOROVÁ J., CHRÁSKA T., VILÉMOVÁ M.: Ultrafine-grained W-Cr composite prepared by controlled W-Cr solid solution decomposition. Materials Letters, 2021.

[IV] VEVERKA J., VILÉMOVÁ M., LUKÁČ F., KADZIELAWA A. P., LEGUT D., VONTOROVÁ J., KOZLÍK J., CHRÁSKA T.: Decreasing the W-Cr solid solution decomposition rate: theory, modelling and experimental verification. Journal of Nuclear Materials, 2023.

Appendix A3 – List of other author´s publications

[V] MATĚJÍČEK J., VEVERKA J., NEMANIČ V., CVRČEK L., LUKÁČ F., HAVRÁNEK V., ILLKOVÁ K.: Characterization of less common nitrides as potential permeation barriers. Fusion Engineering and Design, 2019.

[VI] MATĚJÍČEK J., MUŠÁLEK R., VEVERKA J.: Materials and processing factors influencing stress evolution and mechanical properties of plasma sprayed coatings. Surface and Coatings Technology, 2019.

[VII] HEUER S., MATĚJÍČEK J., VILÉMOVÁ M., KOLLER M., ILLKOVÁ K., VEVERKA J., WEBER T., PINTSUK G., COENEN J.W., LINSMEIER Ch.: Atmospheric plasma spraying of functionally graded steel/tungsten layers for the first wall of future fusion reactors. Surface and Coatings Technology, 2019.

[VIII] MATĚJÍČEK J., VILÉMOVÁ M., VEVERKA J., KUBÁSEK J., LUKÁČ F., NOVÁK P., PREISLER D., STRÁSKÝ J., WEISS Z.: On the Structural and Chemical Homogeneity of Spark Plasma Sintered Tungsten. Metals, 2019.

[IX] TERENTYEV D., VILÉMOVÁ M., YIN C., VEVERKA J., DUBINKO A., MATĚJÍČEK J.: Assessment of mechanical properties of SPS-produced tungsten including effect of neutron irradiation. International Journal of Refractory Metals and Hard Materials, 2020.

[X] KOLLER M., VILÉMOVÁ M., LUKÁČ F., BERAN P., ČÍŽEK J., HADRABA H., MATĚJÍČEK J., VEVERKA J., SEINER H.: An ultrasonic study of relaxation processes in pure and mechanically alloyed tungsten. International Journal of Refractory Metals and Hard Materials, 2020.

[XI] MATEJÍČEK J., VEVERKA J., YIN C., VILÉMOVÁ M., TERENTYEV D., WIRTZ M., GAGO M., DUBINKO A., HADRABA H.: Spark plasma sintered tungsten – mechanical properties, irradiation effects and thermal shock performance. Journal of Nuclear materials, 2020.

[XII] BIESUZ M., SAUNDERS T. G., VEVERKA J., BORTOLOTTI M., VONTOROVÁ J., VILÉMOVÁ M., REECE M. J.: Solidification microstructures of multielement carbides in the high entropy Zr-Nb-Hf-Ta-Cinfx/inf system produced by arc melting. Scripta Materialia, 2021.

[XIII] CSÁKI Š., LUKÁČ F., HÚLAN T., VEVERKA J., KNAPEK M.: Preparation of anorthite ceramics using SPS. Journal of the European Ceramic Society, 2021.

[XIV] DENG H., BIESUZ M., VILÉMOVÁ M., KERMANI M., VEVERKA J., TYRPEKL V., HU CH., GRASSO S.: Ultrahigh temperature flash sintering of binder-less tungsten carbide within 6 s. Materials, 2021.

[XV] CSÁKI Š., LUKÁČ F., VEVERKA J., CHRÁSKA T.: Preparation of Ti_3SiC_2 MAX phase from Ti, TiC, and SiC by SPS. Ceramics International, 2022.

[XVI] OYEDEJI A., OBADA D., DAUDA M., KUBURI L., CSÁKI Š., VEVERKA J.: Fabrication and characterization of hydroxyapatite-strontium/polylactic acid composite for potential applications in bone regeneration. Polymer Bulletin, 2022.